

Editor

Dear Dr. West,

Thank you for submitting your work to *Climate of the Past*, and for your pre-responses to referees' comments. As you had already examined, both referees indicated the importance of the study. They also raised some issues that would require your consideration through a revision. I am looking forward to receiving the revised version.

All the best
Zhengtang GUO
Editor, *Climate of the Past*

Author Reply: Thank you for your comment. We have revised the manuscript according to our initial responses (detailed below), and have not deviated from our initial responses. In addition to these requested revisions we have corrected some minor oversights not encountered during the review process. Revisions have been tracked on the revised manuscript as required in order to facilitate correlation with our responses to reviewers.

We thank Suzanne Leroy for her review and supportive comments on our manuscript. Below we respond to Dr Leroy's comments.

1. Comments to the text Line 149 and others: in calls to fig. 1, precise if A, B, C or D

Author reply: Thank-you for directing our attention to the need to have more specificity in our figure calls; these have been corrected.

2. Lines 297, 301, and others: between xx and xx. Make sure to add an "and".

Author reply: Thank you for the suggestion; however, we followed the Instructions to Authors for *Climate of the Past* that directs authors to use the en dash for ranges of values, e.g. "En dashes are used to indicate, among other things, ... ranges (e.g. 12–20 months), ...".

3. Line 44, and others: from xx to xx

Author reply: Please see our response above.

4. Section 4.1: Write a sentence to remind us why you believe the ensemble is better than the two other methods.

Author reply: The ensemble approach combines all of the proxies. We have added two sentences where indicated to reiterate the improvement the ensemble (of all the proxies) provides over the individual proxies.

5. Comments to the figures and tables Fig. 2 caption: explain abbreviations such as Mbr and Fm (no full stop at the end as it is a contraction, not an abbreviation) Fig. 2: Give units to vertical axis and 3rd column.

Author reply: Thank you for spotting these minor oversights; we have corrected the absence of units on figure 2 and explained the contractions in the figure caption.

6. Fig. 3: it would help the reader if you could plot on a map the locations of the met stations used here.

Author reply: We have added an inset map of North America to figure 3 to address this.

7. Fig. 4B: it is too small, think of making it full page width

Author reply: We have edited figure 4 in order to make 4B larger and more readable.

8. Table 1: give units to latitude, i.e. N° Table 2 caption: explain abbreviations: WA, BC, AL, NU

Author reply: We have added the units for all latitude entries in the table and have added the meanings of the abbreviations to the Table caption.

We thank Lydie Dupont for her review and supportive comments on our manuscript. Below we respond to Dr Dupont's comments.

1. An important reason to study the Eocene is its high levels of atmospheric carbon dioxide. Please mention this aspect in the beginning of the Introduction.

Author Response: We have added some text (new lines 36, and 61–64) to the introduction regarding the broader importance of studying the early Eocene, including elevated CO₂ levels, and how it informs us of the global response of physical and biological systems to global climate change.

2. I think that the more general readership of CP would need a little bit more explanation about the data. I assume that the data include only macro fossils, i.e. leaves, but this is nowhere explicitly stated. This is necessary because the BA-analysis is based on NLR-analysis, which is normally used with pollen data. If the BA-analysis is based on pollen data too, that fact should be mentioned and discussed as the taphonomy of pollen data differs strongly from that of fossil leaves.

Author Response: Our study indeed uses only data sourced from fossil megaflora; however, we do compare our data to some prior studies from contemporaneous high latitude sites that were based on pollen (Table 3). We have added a statement to section 2.1 Fossil Plant Localities that clearly explains to the reader that the data for our study were sourced from fossil megaflora.

3. It also would be helpful to mention which taxa are dominant/important in the assemblages of the sites described.

Author Response: Fossil megafloras from 19 different localities from Washington, British Columbia, Alaska, and the Canadian Arctic were used for this study. In our view, providing a site to site list of dominant taxa would not improve upon the manuscript. Instead, this would serve only to highlight: (1) a number of common taxa that can be found across all sites and which serve to link the polar broad-leaf forests of the high latitudes with the coniferous deciduous forests of the middle latitudes; and, (2) that various taphonomic factors are, as expected, at work across a broad range of sites over a broad latitudinal range that modulate differences between fossil assemblages. We feel it would be more appropriate, and in keeping with the focus of the paper, to explain more clearly in the text that the assemblage data can

be found in the supplied references, where each of these sources list and discuss the assemblages in detail. The text has been modified in sections 2.1.2, 2.1.3, 2.1.4, and 2.1.5 to reflect these additions.

4. It is not clear if the new work in this study concerns the statistical analysis only, or that also new botanical analysis has been carried out. If new botanical analysis has been carried out, the method section has to be complemented.

Author Response: The reviewer raises an important point. Our study does include data and analyses from previous studies, but also includes new leaf physiognomic analyses of fossil floras from the Canadian Arctic and British Columbia. We have edited the appropriate section (new lines 96–98) in the introduction to more clearly outline for the reader that new *and* existing data are used for our study. In addition, we have provided text to sections 2.3.1 and 2.3.2 that indicates which sites had new analyses conducted for this study.

5. I suggest to change the sequence of section 2.3. Please, explain the physiognomic and bioclimatic analysis first and then the combination of ensemble climate analysis.

Author Response: We agree that this sequence may be more logical. We have edited the text as recommended and place the leaf physiognomic and bioclimatic analysis methods before the explanation of the ensemble climate approach, which is now occurs as section 2.3.3.

6. Please leave out the decimals of the temperature and precipitation estimates as they are obviously not significant.

Author Response: One decimal place is appropriate for temperature, as it correctly indicates the precision of our estimates, the precision of the underlying calibration data, and the uncertainty of the estimates. One decimal for temperature is also consistent with how temperature estimates are reported across multiple research teams for these proxies and, importantly, as used in climate model-proxy comparisons. We have therefore retained one decimal place for temperature. We have, however, removed the decimals in section 3.1 and throughout from the precipitation values, where such precision is not warranted.

7. In the discussion, I miss an important point, which has been already discussed by the first author in an earlier paper (West et al. 2015) but should not be forgotten. The photic regime of the poles (more diffuse summer light than at lower latitudes) might result in bigger leaves and, therefore, precipitation estimates might have been overestimated.

Author Response: We have added a brief statement to section 4.1.3 in the discussion that outlines the influence of this potential bias to precipitation estimates.

8. The tables and Fig. 1 could include more information. Please, indicate in the caption of Fig.1 and also in Table 2 the categories ‘Mid-latitude Upland’ etc. as used in the paper.

Author Response: We have edited the captions for figure 1 and table 2 to include this information. In addition, we have updated the tables and the corresponding captions in the appendices to be more consistent with how localities are listed in previous tables.

9. Please, give a more precise age indication in Table 1 and also give an indication of the ages of the data summarized in Table 3.

Author Response: Precise age data are available for some of the fossil localities used for this study, as they have received considerable attention or are easily accessible; however, some fossil localities do not have precise age data. For this reason, we feel that the ages as listed in Table 1 are as precise as is possible at this time, and sufficiently accurate for the purpose of this study. We agree that ages would aid in the presentation of data in Table 3, and we have added the published ages to this table.

10. Specific Comments:

Lines 110-112: needs a reference; please give an estimate of polar displacement.

Author Response: We have added references to this statement as requested; however, as the estimate of displacement is not uniform from the mid-latitudes to the high-latitudes, and depends on the method and model used to estimate displacement, we feel that adding a specific value (or range of values) would serve only to introduce confusion into our text and would not improve upon our interpretations. We therefore retain only a general statement on polar displacement.

Line 227: Physg3brcAZ is not mentioned in Yang, but mentioned in Jacques et al. 2011.

Author Response: The Physg3brcAZ CLAMP dataset was first mentioned in Wolfe (1993). As the datasets have been subject to improvement over time, Yang et al. (2015) represents the most up-to-date improvement of the CLAMP method, which saw the inclusion of a global dataset, and as such includes a recent review of the methodology behind the datasets themselves. However, we recognize that Yang et al. (2015) does not specifically mention the Physg3brcAZ or GRIDMet3brcAZ datasets employed for our study. We have revised the reference on line 227 to cite not only Yang et al. (2015), but also Yang et al. (2011) – a prior study that discusses the CLAMP Online architecture and specifically discusses the datasets used for this study – as well as the original paper by Wolfe (1993) where the Physg3brcAZ dataset was introduced. Jacques et al. (2011), a study primarily focused on detecting monsoonal climate signals in physiognomic data, does reference the Physg3brcAZ CLAMP dataset; however, this would be an incorrect source to cite in this case, so we have added Yang et al. 2011.

Line 228: GRIDMet3brcAZ: Yang mentions GRIDMetGlobal378_HiRes. Is that the same dataset?

Author Response: GRIDMetGlobal378_HiRes is not the same dataset as GRIDMet3brcAZ. However, please see our above response.

Line 305: 3.1.2 (instead of 3.2.2)

Author Response: We have corrected this. Thank-you for catching this oversight.

Line 433: please, mention the kind of fossil evidence.

Author Response: We have added a short list of fossil examples to section 4.1.4 to the text as requested.

References:

Jacques, F.M., Su, T., Spicer, R.A., Xing, Y., Huang, Y., Wang, W. and Zhou, Z.: Leaf physiognomy and climate: are monsoon systems different? *Glob. Planet. Change*, 76(1–2), 56–62, 2011.

- Wolfe, J.A.: A method of obtaining climatic parameters from leaf assemblages. US Government Printing Office, (No. 2040-2041), 1993.
- Yang, J., Spicer, R.A., Spicer, T.E. and Li, C.S.: 'CLAMP Online': a new web-based palaeoclimate tool and its application to the terrestrial Paleogene and Neogene of North America. *Palaeobio. Palaeoenviron.*, 91(3), 163, 2011.
- Yang, J., Spicer, R.A., Spicer, T.E., Arens, N.C., Jacques, F.M., Su, T., Kennedy, E.M., Herman, A.B., Steart, D.C., Srivastava, G., Mehrotra, R.C., Valdes, P.J., Mehrotra, N.C., Zhou, Z., and Lai, J.: Leaf form – climate relationships on the global stage: An ensemble of characters, *Global Ecol. Biogeogr.*, 24, 1113–1125, 2015.

Paleobotanical proxies for early Eocene climates and ecosystems in northern North America from mid to high latitudes

Christopher K. West¹, David R. Greenwood², Tammo Reichgelt³, Alexander J. Lowe⁴, Janelle M. Vachon², and James F. Basinger¹.

¹ Dept. of Geological Sciences, University of Saskatchewan, 114 Science Place, Saskatoon, Saskatchewan, S7N 5E2, Canada.

² Dept. of Biology, Brandon University, 270-18th Street, Brandon, Manitoba R7A 6A9, Canada.

³ Department of Geosciences, University of Connecticut, Beach Hall, 354 Mansfield Rd #207, Storrs, CT 06269, U.S.A.

⁴ Dept. of Biology, University of Washington, Seattle, WA 98195-1800, U.S.A.

Correspondence to: C.K West (christopher.west@usask.ca)

Abstract. Early Eocene climates were globally warm, with ice-free conditions at both poles. Early Eocene polar landmasses supported extensive forest ecosystems of a primarily temperate biota, but also with abundant thermophilic elements such as crocodilians, and mesothermic taxodioid conifers and angiosperms. The globally warm early Eocene was punctuated by geologically brief hyperthermals such as the Paleocene-Eocene Thermal Maximum (PETM), culminating in the Early Eocene Climatic Optimum (EECO), during which the range of thermophilic plants such as palms extended into the Arctic. Climate models have struggled to reproduce early Eocene Arctic warm winters and high precipitation, with models invoking a variety of mechanisms, from atmospheric CO₂ levels that are unsupported by proxy evidence, to the role of an enhanced hydrological cycle to reproduce winters that experienced no direct solar energy input yet remained wet and above freezing. Here, we provide new estimates of climate, and compile existing paleobotanical proxy data for upland and lowland mid-latitudes sites in British Columbia, Canada, and northern Washington, USA, and from high-latitude lowland sites in Alaska and the Canadian Arctic to compare climatic regimes between mid- and high latitudes of the early Eocene—spanning the PETM to the EECO—of the northern half of North America. In addition, these data are used to reevaluate the latitudinal temperature gradient in North America during the early Eocene, and to provide refined biome interpretations of these ancient forests based on climate and physiognomic data.

1 Introduction

The early Eocene (56–47.8 million years ago) was a globally warm interval in Earth history, which resulted from a warming trend correlated with elevated greenhouse gas levels that began in the late Paleocene (Zachos et al., 2008; Carmichael et al., 2016). This warming was punctuated by a series of episodic hyperthermal events (e.g., the Paleocene-Eocene Thermal Maximum and the Eocene Thermal Maximum 2), which caused global climatic perturbations, and ultimately culminated in the early Eocene Climatic Optimum (EECO) (Zachos et al., 2008; Littler et al., 2014; Laurentano et al., 2015; Westerhold et al., 2018). During the early Eocene, the climate of much of northern North America was warm and wet, with mean annual temperatures (MAT) as high as 20 °C, mean annual precipitation (MAP) of 100–150 cm a⁻¹, mild frost-free winters (coldest month mean temperature >5 °C), and climatic conditions that supported extensive temperate forest ecosystems (e.g., Wing and Greenwood, 1993; Wing, 1998; Shellito and Sloan, 2006; Smith et al., 2012; Breedlovestrout et al., 2013; Herold et al., 2014; Greenwood et al., 2016).

These warm and wet conditions extended poleward in North America, despite extreme photoperiodism, promoting the establishment of temperate forest ecosystems and thermophilic biota (e.g., mangroves, palm trees, and alligators) (Eldrett et al., 2009, 2014; Sluijs et al., 2009; Huber and Caballero 2011; Eberle and Greenwood, 2012; Littler et al., 2014; West et al., 2015, 2019; Salpin et al., 2019), and providing evidence for a shallow latitudinal temperature gradient, in contrast to the much higher gradient of modern North America (Greenwood and Wing, 1995; Naafs et al., 2018). The reconstructed paleoclimatic and biotic similarity between the mid- and high latitudes of Eocene North America may be counterintuitive given the limited photic seasonality of mid-latitude sites and the extreme seasonal photic regime of high-latitude environments. In spite of similar thermal regimes, one would expect that the Arctic ecosystems would have experienced unparalleled abiotic stress from the extended period of winter darkness (West et al., 2015), and, as a result, would have had a substantially different climate and biota from that of contemporaneous mid-latitudes sites. Fossil evidence from both the mid- and high latitudes, however, demonstrate little to no discernable effect.

The early Eocene geological record preserves evidence of biota living during a globally warm “greenhouse” interval with elevated atmospheric CO₂ relative to modern levels and as such, offers an opportunity to explore the global response of physical and biological systems to global climate change (Zachos et al., 2008; Hollis et al., 2019). Fossil plants are among the best proxies for terrestrial paleoclimates, as plants are sessile organisms that interact directly with their environment, and whose phenotype is highly moderated by variables such as temperature, moisture, and atmospheric carbon availability. Despite this, paleobotanical proxy reconstructions of temperature and precipitation are often mismatched with General Circulation Model (GCM) simulation output, and models struggle to reproduce the warm high-latitude regions and reduced latitudinal temperature gradient of the early Eocene as evidenced from the fossil record (Huber and Caballero, 2011; Huber and Goldner, 2012; Herold et al., 2014; Carmichael et al., 2016; Lunt et al., 2017, 2020; Keery et al., 2018; Naafs et al., 2018; Hollis et al., 2019). This suggests that

Deleted: ,

some atmospheric processes related to heat transfer may be missing from GCM simulations (Carmichael et al., 2018, and references cited therein). Furthermore, there are far fewer compilations of terrestrial temperature proxy data as compared to marine-based data compilations of sea surface temperatures (SST) (Hollis et al., 2019). This results in spatial, or geographic, gaps in proxy data—essentially the paucity of data requires that proxy climate data separated by considerable distance must be used to interpolate climate over large geographic areas—that impede the efficacy of GCM simulations (Hollis et al., 2019). However, concerted efforts have been made to fill the geographic gaps through the development of new, targeted compilations and additional proxy data (e.g., DeepMIP, Hollis et al., 2019; Lunt et al., 2020). In addition, models do not typically incorporate potential vegetative feedbacks (Lunt et al., 2012), although advances in defining functional plant types have been made (Loftson et al., 2014).

Therefore, there is a need to refine the quality and consistency of physiognomic and Nearest Living Relative (NLR) paleobotanical proxy data estimates, provide new physiognomic and NLR proxy data to help fill regional and temporal gaps, and provide more reliable forest biome interpretations. An emphasis needs to be placed on multi-proxy studies that evaluate an ensemble of proxy estimates, which allows for identifying strongly congruent paleoclimate proxy reconstructions where the results agree, and inconsistencies where the failures of individual proxy estimates can be identified. Thus, the purpose of this study is to reconsider reported, and introduce new, early Eocene paleobotanical climate data from northern North America utilizing a refined methodology where a bootstrapping approach is applied to the data to produce ensemble climate estimates. Paleobotanical-based paleoclimate reconstructions from northern North America are reviewed, and new paleoclimate estimates are provided for British Columbia and the Canadian Arctic through application of a multi-proxy ensemble approach. Our multi-proxy ensemble analysis utilizes both new and previously published leaf physiognomic, and new nearest living relative data, as recommended by Hollis et al. (2019) and others (e.g., Reichgelt et al., 2018, Lowe et al., 2018; Willard et al., 2019) in order to mitigate potential errors resulting from variations between methods.

Paleobotanical assemblages from four distinct regions in northern North America are considered here: mid-latitude lowland sites; mid-latitude upland sites; low polar lowland sites; and high polar lowland sites. Comparison of lowland sites allows for reevaluation of the terrestrial latitudinal temperature gradient in northern North America. Furthermore, the distribution of vegetation, as potentially moderated by climate, elevation, continentality, and photoperiod is evaluated through comparisons of the mid-latitude upland and high-latitude lowland fossil localities. This is achieved by plotting climate data on biome diagrams, as well as principal component analysis (PCA) and hierarchical cluster analysis (HCA) of leaf physiognomy. This provides a more robust interpretation of these ancient forested ecosystems, which will contribute to refinement of modelling simulations by providing reliable insight for prescribing early Eocene boundary conditions for high latitude vegetation and environments.

2 Materials and Methods

2.1 Fossil plant localities

Early Eocene paleobotanical proxy data [used for this study](#) are sourced from [fossil megaf flora \(i.e., fossil leaves and other organs\) from](#) multiple fossil localities from the northern mid-latitudes (48.3–51.2 °N) and high latitudes (61.4–81.4 °N) of North America, primarily within Canada, but also including sites from Washington State and Alaska (Table 1). In general, the majority of fossil localities used for this study were within a few degrees latitude of their present position, as North America has moved obliquely past the rotational pole since the Eocene ([McKenna 1980; van Hinsbergen et al., 2015](#)). As the resulting slight poleward displacement is not significant for the present work, we report modern latitudes for the compilation of fossil localities within this study to avoid discrepancies in differing methods of estimating paleolatitudes. These localities represent both lowland and upland ecosystems. Prior physiognomic analyses of fossil megaf flora from both the mid-latitudes and high-latitudes of North America indicate that these ancient forests were growing under similar thermal regimes (e.g., MAT 10–15 °C and MAP 100–150 cm a⁻¹) (Wing and Greenwood, 1993; Greenwood and Wing 1995; Smith et al. 2012; West et al., 2015; Gushulak et al., 2016; Greenwood et al., 2016; Lowe et al., 2018). The Canadian fossil localities (e.g., British Columbia and Nunavut) are stratigraphically correlated, placing all the fossil study sites into a chronological sequence spanning the early Eocene (McIver and Basinger 1999; Greenwood et al., 2016; Eberle and Greenwood 2017; West et al., 2019). Other localities within our data set (e.g., Evan Jones Mine, AK, Racehorse Creek, and Republic, WA) are also considered equivalent in age, and the stratigraphic relationships for these floras may be found in the respective publications for these localities (Table 1).

2.1.2 Mid-latitude Upland Fossil Plant Localities

The Okanagan Highlands host a suite of mid-latitude upland fossil floras from British Columbia and Washington (Archibald et al., 2011; Greenwood et al., 2016) (Table 1, Fig. 1d). These fossil localities have been dated radiometrically as early Eocene, likely occurring within the EECO (Moss et al., 2005; Smith et al., 2009; Greenwood et al., 2016; Mathewes et al., 2016; Lowe et al., 2018). Okanagan Highland floras are broadly similar in floristic composition, comprised of a high diversity of plant genera typical of modern temperate deciduous and subtropical evergreen forests (DeVore and Pigg, 2010; Smith et al., 2012; Gushulak et al., 2016; Lowe et al., 2018). [Detailed discussion regarding the composition of the mid-latitude upland fossil floral assemblages can be found in the primary resources describing these fossil sites \(see Smith et al., 2012; Greenwood et al., 2016; Lowe et al., 2018\).](#) These forests were regionally extensive, occupying north-south orientated and arc-related volcanic highlands (Mathewes 1991; Lowe et al., 2018). The paleoelevation of these sites has been reconstructed to be between 500–1500 m based on both paleobotanical and geochemical proxies (Wolfe et al., 1998; Greenwood et al., 2005, 2016; Tribe, 2005; Smith et al., 2012), and as a result of this altitude, these forests would have experienced cooler temperatures than the coastal lowlands to the west (Wolfe et al., 1998; Greenwood et al., 2016; Lowe et al., 2018). In addition to plants, fossil insect diversity is high, similar to modern-day tropical forests (Archibald et al., 2010, 2013)

Deleted:

2.1.3 Mid-latitude Lowland Fossil Plant Localities

The uppermost Paleocene to middle Eocene Chuckanut Formation of western Washington State (Fig. 1c) contains several fossil floras representing subtropical coastal lowland ecosystems, including palms and many other thermophilic plant taxa (Breedlovestrout et al., 2013; Mathewes et al., 2020). The Chuckanut floras used for this study are the Racehorse Creek fossil localities, which are found within the Slide Member (Fig. 2), a thick terrestrial deposit that has been radiometrically dated to the early Eocene (Breedlovestrout et al. 2013). [See Breedlovestrout et al. \(2013\) for additional details regarding the composition of the Chuckanut fossil megaf flora assemblage.](#)

2.1.4 High-latitude Low Polar Lowland Fossil Localities

The Chickaloon Formation in south-central Alaska (Fig. 1c) preserves a fossil flora known from the Evan Jones Mine (Sunderlin et al., 2011), herein referred to as the Evan Jones Mine flora. Wolfe et al. (1966) assigned a Paleocene age to the Chickaloon Formation based on K-Ar dating. However, fission-track zircon dating shows that the Paleocene-Eocene boundary occurs within the upper 150 m of the Chickaloon Formation (Triplehorn et al., 1984), stratigraphically near the fossil flora (Fig. 2), and therefore the Chickaloon Formation straddles the Paleocene-Eocene boundary (*sensu* Sunderlin et al., 2011). The Evan Jones Mine flora represents a lowland warm temperate to subtropical floodplain forest, as fossil palms are present and a high proportion of the flora exhibits leaves with untoothed margins (Wolfe et al., 1966; Sunderlin et al., 2011). [See Sunderlin et al. \(2011\) for additional details regarding the composition of the Evan Jones Mine fossil megaf flora assemblage.](#)

2.1.5 High-latitude High Polar Lowland Fossil Localities

Fossil floras from Ellesmere and Axel Heiberg islands in Nunavut, Canada, are the most northerly fossil sites included in this study (Fig. 1b). These fossil floras have been sampled extensively from formations within the Eureka Sound Group, primarily from the Mount Lawson, Mount Moore, and Margaret (=Iceberg Bay) formations (Fig. 2) (McIver and Basinger, 1999; West et al., 2019). The Margaret Formation at Stenkul Fiord and the Mount Lawson Formation at Split Lake have been radiometrically dated to the early Eocene (Reinhardt et al., 2013, 2017). Additional age controls (i.e. vertebrate fossils, palynology, paleomagnetic dating) suggest either late Paleocene, early Eocene, or both for all three formations at various localities (Eberle and Greenwood, 2012; West et al., 2019). The fossil floras of the Canadian Arctic are therefore considered to represent the late Paleocene to early Eocene time interval, with some localities capturing the PETM and ETM-2 hyperthermal events (e.g., Stenkul Fiord) (Sudermann et al., in review). These high-latitude fossil floras represent lowland environments and are considered warm temperate floodplain or swamp forests (McIver and Basinger, 1999; Greenwood et al., 2010; West et al., 2019). Although this high-Arctic assemblage as a whole is of a high taxonomic richness (see West et al., 2019), the site-to-site diversity (β diversity) is the lowest within the compilation for

Deleted: ,

Deleted: 3.

this study. [See West et al. \(2019\) for a detailed discussion regarding the composition of the high-latitude polar lowland fossil megaflora assemblages.](#)

Deleted: se

2.2 Sampling

At the majority of the fossil sites from British Columbia, fossil leaves were comprehensively sampled along bedding planes, using census sampling (i.e. collecting >300 leaf morphotype specimens; Wilf, 2000; Lowe et al., 2018). Some sites, such as those from the Canadian Arctic (i.e., Ellesmere and Axel Heiberg islands) and others from British Columbia (i.e., Chu Chua, Driftwood Canyon, One Mile Creek, Thomas Ranch), represent leaf collections from prior work by earlier researchers where sampling was selective to yield a representative sample of the leaf taxa present. Some localities reported in this study were not sampled by the authors (e.g., Evan Jones Mine, Alaska; Chu Chua, One Mile Creek, Quilchena and Thomas Ranch, BC; Racehorse Creek and Republic, WA), therefore, the details of the sampling protocols for those floras may differ from sampling methods outlined above. The sampling methods for those fossil sites can be found in their original respective publications (Table 1).

Deleted: ,

2.3 Paleoclimate Analyses

2.3.1 Leaf Physiognomy

Leaf physiognomy methods, such as Climate Leaf Analysis Multivariate Program (CLAMP) and Leaf Area Analysis (LAA), utilize correlations between leaf architecture and climate variables derived from modern global vegetation databases to provide estimates of paleoclimate variables (Greenwood, 2007; Peppe et al., 2011; Yang et al., 2015; Hollis et al., 2019). Hollis et al. (2019) noted the potential for disparity between fossil plant-based climate proxies and calibrations within individual proxies that can contribute to differences in climate estimates, and as such represent a challenge for model-data comparisons for the Eocene.

We primarily report physiognomically derived paleoclimate estimates from CLAMP, as these were readily available from some localities from prior studies (e.g., Wolfe et al., 1998; Sunderlin et al., 2011; Smith et al., 2012; Breedlovestrout et al., 2013; Dillhoff et al., 2013; West et al., 2015; Gushulak et al., 2016; Mathews et al., 2016; Lowe et al., 2018), and because CLAMP provides estimates of seasonal temperatures and precipitation. The use of CLAMP estimates allows comparisons between the paleontological proxy estimates of winter temperatures and the seasonality of precipitation with climate model output, parameters that are of interest in understanding early Eocene climates at mid- and high latitudes (Huber and Caballero, 2011; Huber and Goldner, 2012; Carmichael et al., 2016; Hollis et al., 2019). For sites where the original published CLAMP estimates were incomplete or run early in the development of CLAMP (e.g., Chu Chua, One Mile Creek and Republic; Wolfe et al., 1998), we have re-run the CLAMP analyses using the original score sheets archived on the CLAMP online website. The Physg3brcAZ vegetation and the GRIDMet3brcAZ meteorological datasets were used for the analyses run for

Moved down [1]: 2.3.1 Ensemble Climate Analysis¶

We apply an ensemble climate analysis approach that avoids choosing one method over another, so that we can present the results from each method as well as the consensus reconstruction based on all methods (Greenwood, 2007; Gushulak et al., 2016; Greenwood et al., 2017; Lowe et al., 2018; Willard et al., 2019; Hollis et al., 2019). The ensemble approach also highlights potential disparity between different proxy reconstructions. This approach is applied to both physiognomic and bioclimatic analysis (BA) climate data compilations (see below). Statistically assessed ensemble estimates of Mean Annual Temperature (MAT), Coldest Month Mean Temperature (CMMT), Warmest Month Mean Temperature (WMMT), and Mean Annual Precipitation (MAP) were produced by bootstrapping results of high mid-latitude and high-latitude fossil site physiognomic and BA data. The mean and standard deviations were resampled using $n=1000$ Monte Carlo simulations for each proxy reconstruction at each site. A probability density function was then calculated for each climatic variable, for each site. The BA-based summer mean temperature (ST) and winter mean temperature (WT) estimates (see section 2.3.3 below for a discussion of these terms) were transformed to WMMT and CMMT, respectively, using a method described in Reichgelt et al. (2018), wherein a linear regression function between ST and WMMT, and WT and CMMT is used to calculate values in NLR that can be directly compared to physiognomic proxy results (Figure A1). This method is in line with the recommendations of Hollis et al. (2019), where a statistically-assessed multi-proxy consensus approach should be utilized when feasible for reconstructing terrestrial climate.¶

Deleted: 2

this study (Wolfe, 1993; Yang et al., 2011, 2015). For CLAMP estimates sourced from existing studies, the vegetation and meteorological datasets are reported in those sources (Table 1).

The estimates from CLAMP are supplemented with estimates using leaf area analysis (LAA) for mean annual precipitation (Wilf et al., 1998; Peppe et al., 2011) a climate parameter not typically provided by CLAMP, as well as leaf margin analysis (LMA) for mean annual temperature (Wilf, 1997; Greenwood, 2007; Peppe et al., 2011). Estimates for Falkland, Quilchena and Thomas Ranch in British Columbia, Evan Jones Mine in Alaska, and three sites from Ellesmere Island in Nunavut are reported from the original analyses of those localities (Wolfe et al., 1998; Breedlovestrout, 2011; Smith, 2011; Sunderlin et al., 2011; Smith et al., 2012; Breedlovestrout et al., 2013; Dillhoff et al., 2013; West et al., 2015), but are supplemented with previously unreported CLAMP, LAA, and LMA paleoclimate estimates (Table A1 & A2) from British Columbia (i.e., Whipsaw Creek) and the Canadian Arctic (i.e., Strand Fiord, Fosheim Anticline, Hot Weather Creek, Mosquito Creek, Ox Head Creek).

2.3.2 Bioclimatic Analysis

In addition to physiognomic analyses, we employ Bioclimatic Analysis (BA) (Greenwood et al., 2005), which extracts paleoclimatic information from fossil assemblages based on the modern-day distribution of nearest living relatives (NLR) of the taxa found in the fossil assemblage. New paleoclimate estimates from BA were produced for all fossil localities used for this study (Table A3). Here, BA was performed by calculating probability density functions (e.g., Greenwood et al., 2017; Hyland et al., 2018; Willard et al., 2019) for each site and each climatic variable: mean annual temperature (MAT), summer mean temperature (ST), winter mean temperature (WT) and mean annual precipitation (MAP).

ST and WT represent the average temperature for the three warmest and coldest months, respectively. This is in contrast with warm month mean temperature (WMMT) and cold month mean temperature (CMMT) output of CLAMP, which represent the mean temperature during the warmest and coldest month, respectively. This is the result of the gridded climate data used in these approaches; BA relies on Hijmans et al. (2005), whereas CLAMP relies on gridded climate data of New et al. (2002). Modern-day plant distributions were derived from the Global Biodiversity Information Facility, which were then cross-plotted with gridded climatic maps using the 'dismo' package in R (Hijmans et al., 2005) in order to calculate means (μ) and standard deviation (σ) for each taxon and each climatic variable. The geodetic records were first filtered in order to remove recorded occurrences with uncertain taxonomic assignments, as well as exotic and duplicate occurrences. Additionally, a random subset of the geodetic data was created that filtered out all but three occurrences in every $0.1^\circ \times 0.1^\circ$ gridcell and all but 10 in every $1^\circ \times 1^\circ$ gridcell. This is to avoid overrepresentation of oversampled regions of the world.

Grimm and Potts (2016) pointed out that assessing the bioclimatic range of plant taxa for each climatic variable separately may create an 'apparent bioclimatic envelope', where none of the occurrences fall within a certain combination of temperature and precipitation, but the climatic

Moved (insertion) [2]

Deleted: some of these localities

Moved up [2]: (Wolfe et al., 1998; Breedlovestrout, 2011; Smith, 2011; Sunderlin et al., 2011; Smith et al., 2012; Breedlovestrout et al., 2013; Dillhoff et al., 2013; West et al., 2015)

Deleted: 3

combination is still possible due to this apparent overlap. To circumvent this problem, we assess the likelihood (f) of a taxon (t) occurring at a combination of climatic variables, in this case MAT, ST, WT and MAP.

$$f(t_n) = \left(\frac{1}{\sqrt{2\sigma_{MAT}^2\pi}} e^{(x_{MAT}-\mu_{MAT})^2/2\sigma_{MAT}^2} \right) \times \left(\frac{1}{\sqrt{2\sigma_{ST}^2\pi}} e^{(x_{ST}-\mu_{ST})^2/2\sigma_{ST}^2} \right) \times \left(\frac{1}{\sqrt{2\sigma_{WT}^2\pi}} e^{(x_{WT}-\mu_{WT})^2/2\sigma_{WT}^2} \right) \times \left(\frac{1}{\sqrt{2\sigma_{MAP}^2\pi}} e^{(x_{MAP}-\mu_{MAP})^2/2\sigma_{MAP}^2} \right) \quad (1)$$

Any combination of climatic variables can be assessed in this way. The likelihood of each taxon is then combined to create an overall probability density function (z) for each climatic variable representative of the most likely bioclimatic range of the taxa in the assemblage.

$$f(z) = f(t_1) \times f(t_2) \times \dots \times f(t_n) \quad (2)$$

This method creates highly variable probability densities, dependent on both the number of taxa and the disparity of the climatic range of the NLR's. The climatic values reported here represent the value with the highest absolute probability, and the 95% Confidence Interval represents the minimum and maximum values at which the absolute probability was $\geq 5\%$ the maximum probability.

2.3.3 Ensemble Climate Analysis

We apply an ensemble climate analysis approach that avoids choosing one method over another, so that we can present the results from each method as well as the consensus reconstruction based on all methods (Greenwood, 2007; Gushulak et al., 2016; Greenwood et al., 2017; Lowe et al., 2018; Willard et al., 2019; Hollis et al., 2019). The ensemble approach also highlights potential disparity between different proxy reconstructions. This approach is applied to both physiognomic and BA climate data compilations (see above). Statistically assessed ensemble estimates of Mean Annual Temperature (MAT), CMMT, WMMT, and Mean Annual Precipitation (MAP) were produced by bootstrapping results of high mid-latitude and high-latitude fossil site physiognomic and BA data. The mean and standard deviations were resampled using $n=1000$ Monte Carlo simulations for each proxy reconstruction at each site. A probability density function was then calculated for each climatic variable, for each site. The BA-based ST and WT estimates were transformed to WMMT and CMMT, respectively, using a method described in Reichgelt et al. (2018), wherein a linear regression function between ST and WMMT, and WT and CMMT is used to calculate values in NLR that can be directly compared to physiognomic proxy results (Figure A1). This method is in line with the recommendations of Hollis et al. (2019), where a statistically assessed multi-proxy consensus approach should be utilized when feasible for reconstructing terrestrial climate.

Moved (insertion) [1]

Deleted: 1

Deleted: bioclimatic analysis (

Deleted:)

Deleted: below

Deleted: Coldest Month Mean Temperature (

Deleted:)

Deleted: Warmest Month Mean Temperature (

Deleted:)

Deleted: summer mean temperature (

Deleted:)

Deleted: winter mean temperature (

Deleted:)

Deleted: (see section 2.3.3 below for a discussion of these terms)...

Deleted: -

358 **2.4 Biome and Physiognomic Character Analysis**

359 The physiognomic, BA, and ensemble climate estimates of each fossil locality were plotted on a
360 Whittaker (1975) biome diagram, modified from Woodward et al. (2004), in order to determine
361 the corresponding modern biome classification for each paleoforest based on paleoclimatic
362 estimates. In addition, the CLAMP derived physiognomic data for each fossil locality were
363 analyzed using principal component analysis (PCA) against a comprehensive global compilation
364 of modern physiognomic data (Yang et al., 2015; Hinojosa et al., 2011; Reichgelt et al., 2019) to
365 determine the most similar modern physiognomic analogues of the fossil sites. Finally, the
366 physiognomic characteristics of fossil, and a subset of modern, sites were compared using a
367 hierarchical cluster analysis to determine similarity. This was achieved by calculating a Euclidean
368 dissimilarity matrix without scaling using the "cluster" package in R (Maechler et al. 2019) and
369 the "Ward D2" method for Hierarchical Clustering (R Core Team, 2019).

Deleted: of

370 **3 Results**

371 3.1 Quantitative paleoclimate analysis from paleobotanical proxies

372 3.1.1 Mid-latitude Upland Fossil Plant Localities

373 Ensemble estimates of MAT for the mid-latitude upland fossil localities of British
374 Columbia and Washington ranged between 7.0–14.9 °C, with the range of mean temperatures for
375 the coldest (CMMT) and warmest months (WMMT) between -0.3–4.3 °C and 18.6–22.7 °C,
376 respectively (Table 2). Ensemble MAP estimates for these localities ranged between 80–135 cm
377 a⁻¹ (Table 2), while CLAMP estimates for the three wettest and three driest months (3WET and
378 3DRY) for these localities ranged between 40–66 cm (error ± 23 cm) and 12–29 cm (error ± 6
379 cm), respectively (Table A1). The complete compilation of site-specific physiognomic and BA
380 data for mid-latitude upland fossils sites of British Columbia and Washington is provided in tables
381 A1–A3.

Deleted: .0

Deleted: .1

Deleted: 11

Deleted: .5

Deleted: 8.9

Deleted: 2

382 3.1.2 Mid-latitude Lowland Fossil Plant Locality

383 Ensemble estimates of MAT for the mid-latitude lowland Racehorse Creek fossil sites from
384 western Washington ranged between 17.3–18.9 °C, with the mean temperatures for the coldest
385 (CMMT) and warmest months (WMMT) between 7.3–11.4 °C and 23.1–23.6 °C, respectively
386 (Table 2). The ensemble MAP estimate for Racehorse Creek was 135 cm a⁻¹ (Table 2), while
387 CLAMP estimates for the three wettest and three driest months (3WET and 3DRY) for this locality
388 were 59 cm (error ± 23 cm) and a range of 23–26 cm (error ± 6 cm), respectively (Table A1). The
389 complete compilation of site-specific physiognomic and BA data for Racehorse Creek is provided
390 in tables A1–A3.

Deleted: 8.7

Deleted: .4

Deleted: 5.9

391 3.1.3 High-latitude Low Polar Lowland Fossil Locality

402 Ensemble estimate of MAT for the Chickaloon Formation Evan Jones Mine fossil flora
403 was 13.7 °C, with estimates of CMMT and WMMT of 6.4 °C and 21.8 °C, respectively (Table 2).
404 The ensemble MAP estimate for the Evan Jones Mine flora was 132 cm a⁻¹ (Table 2), while
405 reported CLAMP estimates for the three wettest and three driest months (3WET and 3DRY) from
406 Sunderlin et al. (2011) for this locality were 64 cm (error ± 23 cm) and 37 cm (error ± 6 cm),
407 respectively (Table A1). The complete compilation of site-specific physiognomic and BA data of
408 the Evans Jones Mine flora from Alaska is provided in tables A1–A3.

Deleted: 3.5

Deleted: 6.6

409
410 3.1.4 High-latitude High Polar Lowland Fossil Localities

411 Ensemble estimates of MAT for the high-latitude fossil localities from Arctic Canada
412 ranged from 7.6–12.9 °C, with the range of CMMT and WMMT from 1.3–4.2 °C and 18.2–22.2
413 °C, respectively (Table 2). Ensemble MAP estimates for Ellesmere and Axel Heiberg islands
414 ranged between 131–180 cm a⁻¹ (Table 2), while CLAMP estimates for the three wettest and three
415 driest months (3WET and 3DRY) for the Arctic Canada fossil localities ranged between 37–54 cm
416 (error ± 23 cm) and 20–31 cm (error ± 6 cm), respectively (Table A1). The complete compilation
417 of site-specific physiognomic and BA data for Ellesmere and Axel Heiberg islands fossil plant
418 localities is provided in tables A1–A3. In addition, climate estimates for Lake Hazen are produced
419 using BA (Table A3), as taxonomic data for this site recently became available (West et al., 2019).
420 Lake Hazen represents the most northerly (~81 °N) terrestrial plant fossil sites available in North
421 America and as such, climate data from this site help fill important geographic gaps. Although the
422 number of broadleaf taxa identified at this locality (*n* = 11) was comparable to other Ellesmere
423 Island fossil localities (e.g., Split Lake), many specimens were fragmentary and incomplete. This
424 limited the number of taxa that could be reliably scored to an insufficient number (*n* = 6) to run
425 leaf physiognomic analyses with meaningful precision and accuracy (Greenwood, 2007; Peppe et
426 al., 2011; Yang et al., 2015), and as such this site could not be included in the site-specific
427 ensemble analysis.

Deleted: 6.9

Deleted: .4

Deleted: 19.7

Deleted: .3

Deleted: ,

428 3.2 Biome types, Principal Component Analysis (PCA), and Hierarchical Cluster Analysis
429 (HCA) using leaf physiognomy

430 The ensemble climate data for all fossil localities plotted within the temperate forest space;
431 however, the high polar lowland Arctic sites plot along the boundary between temperate forest and
432 temperate rainforest (Fig. 3a). The mid-latitude lowland and upland fossil sites, as well as the low
433 polar lowland site from Alaska, plotted as temperate forests using the physiognomic climate
434 estimates from CLAMP and LAA (Fig. 3b). The high polar lowland fossil localities plot as
435 temperate rainforests when the CLAMP and LAA climate estimates are plotted on biome diagrams
436 (Fig. 3b). However, when the BA climate data are plotted, all fossil localities plot closely within
437 the temperate forest space (Fig. 3c). Results from PCA show that the mid-latitude upland and the
438 Canadian Arctic fossil localities generally plot with modern North American floras (Fig. 4b). The
439 HCA, however, shows the high polar Arctic floras, which group on their own branch, to be
440 dissimilar from modern North American floras (Fig. 4c), whereas the mid-latitude upland floras

Deleted: Plotting t

Deleted: a

Deleted: b

451 share some physiognomic characteristics with both the Arctic fossil floras and modern floras from
452 the North American west coast (e.g., Oregon, Washington), and east coast (e.g., Florida, South
453 Carolina). The physiognomic datasets of the Racehorse Creek fossil flora from western
454 Washington and Evan Jones Mine Alaska are not published, and as such were not included in the
455 PCA and HCA analyses of leaf physiognomy.

456 **4. Discussion**

457 **4.1 Climate Reconstruction**

458 The ensemble climate analysis approach provides a consensus reconstruction based on all proxy
459 methods utilized for the paleoclimate reconstruction (Lowe et al., 2018; Willard et al., 2019; Hollis
460 et al., 2019). The ensemble approach has two advantages: (1) it avoids preferentially choosing one
461 method over another by combining the results from all methods to produce a statistically robust
462 assessment; and (2) disparate, potentially anomalous values produced by competing methods are
463 muted as a result of the ensemble approach.

464 **4.1.1 Mid-Latitude Upland Climate Reconstruction**

465 The ensemble MAT estimates of 7.0–14.9 °C correlate with a cooler to warm temperate
466 climate and agree with previous studies of these upland paleofloras of British Columbia and
467 Washington (Greenwood et al., 2005, Smith et al., 2011; Greenwood et al., 2016; Lowe et al.,
468 2018). However, temperatures below 10 °C imply winters that would have experienced periods of
469 sustained frost, a climate feature that is inconsistent with fossil data (Greenwood et al., 2016). The
470 mean of ensemble MAT estimates, however, suggests an average regional temperature for the
471 Okanagan Highlands of ~10 °C, and is more in line with fossil evidence from previous studies
472 (Archibald et al., 2014; Greenwood et al., 2016). The mean ensemble CMMT and WMMT
473 estimates indicate regional temperatures of ~2 °C and ~20 °C, respectively. These estimates
474 suggest that the mid-latitude upland regions in British Columbia and Washington experienced mild
475 winter temperatures (>0 °C) and moderate seasonal changes in temperature. The mean of the
476 ensemble MAP estimates for the Okanagan Highlands suggests an average precipitation of ~110
477 cm a⁻¹, which indicates mesic conditions (MAP >100 cm a⁻¹), and aligns with fossil evidence that
478 suggests these high-altitude forests were wet-temperate ecosystems (Greenwood et al., 2016).
479 These temperature and precipitation estimates, as well as the compilation of climate data (Table 2
480 and Tables A1–A3), indicate that the upland regions of British Columbia and Washington
481 experienced a climate during the Eocene similar to the modern day North Pacific coast of North
482 America (e.g., from Vancouver, British Columbia MAT 10.1 °C, CMMT 3.3 °C, WMMT 17.6 °C,
483 MAP 120 cm a⁻¹, 3WET 51 cm, 3DRY 13 cm, Environment Canada, 2020; to Portland, Oregon
484 MAT 11.7 °C, CMMT 4.6 °C, WMMT 19 °C, MAP 119 cm a⁻¹, 3WET 47 cm, 3DRY 10 cm,
485 NOAA, 2020).

Deleted: s

Deleted:

Deleted: .2

Deleted: ;

Deleted: .2

491 In some cases, site-specific leaf physiognomic-based estimates of MAT were significantly
 492 lower than nearby MAT estimates from contemporaneous neighboring fossil localities, and are
 493 considered anomalous (e.g., LMA estimates of MAT 2.4 °C from One Mile Creek, B.C. see Table
 494 A2). However, as a result of applying our ensemble approach, these anomalous values are muted,
 495 as that particular proxy estimate is not weighed as heavily. It is important to note that the early
 496 Eocene Okanagan Highland floras of British Columbia and Washington were upland ecosystems;
 497 as such, these higher elevation ecosystems would have experienced cooler temperatures than the
 498 neighboring lowland fossil localities (e.g., Racehorse Creek) due to temperature lapse with altitude
 499 (Wolfe et al., 1998; Smith et al., 2009, 2012; Greenwood et al., 2016; Lowe et al., 2018).

Deleted: proxy

501 4.1.2 Mid-latitude Lowland Climate Reconstruction

502 The ensemble MAT estimates of 17.3–18.9 °C from the lowland Racehorse Creek fossil
 503 localities in western Washington indicate a significantly warmer temperature regime compared to
 504 the nearby Okanagan Highland upland floras. These MAT estimates, as well as the ensemble
 505 CMMT estimates of 7.3–11.4 °C, for Racehorse Creek are in line with thermophilic fossil evidence
 506 from the region, including coryphoid palm leaf fossils found in the Chuckanut and Huntingdon
 507 formations (Breedlovestrout et al., 2013; Greenwood and Conran, 2020). The palm tribe
 508 Coryphoideae, while somewhat cold hardy, is restricted (-2σ) to climates with MAT ≥ 10.3 °C and
 509 CMMT ≥ 3.9 °C (Reichgelt et al., 2018). The most recent investigations of the Racehorse Creek
 510 fossil flora reported a MAP estimate of 250–360 cm a⁻¹ (see Breedlovestrout et al., 2013 and
 511 references therein). This is considerably wetter than our ensemble MAP estimate of 135 cm a⁻¹ or
 512 even the upper 95% confidence interval value of 183 cm a⁻¹ (Table 2). These ensemble estimates
 513 should potentially be considered as minimum MAP values, as the Racehorse Creek floras were
 514 lowland coastal environments (Breedlovestrout et al., 2013), and may have experienced more
 515 precipitation than estimated here. The compilation of estimated climate data (Table 2 and Tables
 516 A1–A3) suggests the lowland regions of western Washington experienced a warm and wet climate
 517 during the Eocene similar to regions of the southeast of North America (e.g., Augusta, Georgia,
 518 MAT 18.4 °C, CMMT 9.2 °C, WMMT 26.0 °C, MAP ~118 cm a⁻¹, 3WET 36 cm, 3DRY 26 cm,
 519 NOAA, 2020).

Deleted: 2019

Deleted: .8

Deleted: .5

520 4.1.3 High-Latitude Low Polar Climate Reconstruction

521 The ensemble MAT estimates of 13.3 °C for the Evan Jones Mine flora align with previous
 522 studies (e.g., Sunderlin et al., 2011) that indicated these low polar lowland floras were growing
 523 under a cooler to warm temperate climate, and similar to a MAT (12.3 °C) estimate by Wolfe
 524 (1994). Previously, MAP of the Evan Jones Mine flora had been estimated to be 155 cm a⁻¹
 525 (Sunderlin et al., 2011). Our ensemble estimate for MAP of 132 cm a⁻¹ is a little drier than these
 526 prior estimates; however, the upper bound of the 95% confidence interval for the ensemble MAP
 527 estimates suggests precipitation could have been considerably wetter (367 cm a⁻¹, Table 2). The

Deleted: 4.6

ensemble MAT and MAP estimates, coupled with the ensemble CMMT (6.4 °C) and WMMT (21.8 °C) estimates indicate that Alaska experienced some thermal seasonality, mild winter temperatures (>0 °C), and typically wetter conditions than the mid-latitude upland floras of the Okanagan Highlands, but drier than the coastal lowland Racehorse Creek site. The early Eocene climate reconstruction for Alaska is considerably different from the modern-day climate of Alaska, as modern Alaska experiences a cold and dry climate (e.g., Anchorage, AK MAT 2.8 °C, CMMT -8.2 °C, WMMT 14.9 °C, MAP 42 cm a⁻¹, 3WET 21 cm, 3DRY 5 cm; NOAA, 2020).

4.1.4 High-latitude High Polar Climate Reconstruction

The range of ensemble MAT estimates of 7.6–12.9 °C for the Canadian High Arctic sites agree with previous estimates that indicated these polar lowland floras were growing under a cooler to warm temperate climate. However, similar to the MAT estimates for the upland Okanagan Highland floras, the cooler range of MAT estimates (< 10 °C), would suggest that these high-latitude forests would have experienced periods of sustained frost, an interpretation inconsistent with fossil evidence (e.g., alligators, tortoises, *Glyptostrobus*, and plants possibly affiliated with the tropical monocot family *Strelitziaceae*; see McIver and Basinger, 1999; Eberle and Greenwood et al., 2012; West et al., 2019 for additional details). The mean of the ensemble MAT estimates of ~10 °C, however, is a more in line with the other proxy evidence for a MAT minimum of the polar regions during the early Eocene, and is a thermal regime supported by fossil evidence mentioned above (McIver and Basinger, 1999; Eberle and Greenwood, 2012; West et al., 2019).

The mean values of the ensemble CMMT and WMMT estimates, ~3 °C and ~18 °C respectively, indicate that the Canadian Arctic experienced moderate thermal seasonality and mild winter temperatures (>0 °C). Previously, MAP for three fossil localities from Ellesmere Island had been estimated to be > 200 cm a⁻¹ (e.g., West et al., 2015). New physiognomic estimates of MAP for additional sites from Ellesmere and Axel Heiberg islands produced somewhat drier estimates (~175 cm a⁻¹, Table A2). The ensemble MAP estimates for the Canadian Arctic, ranging from 131–180 cm a⁻¹, with a mean value of 162 cm a⁻¹ (Table 2), are also drier than the West et al. (2015) physiognomic estimates. These MAP values, though drier than the most recent physiognomic estimates, are still indicative of a wet climate similar to, or wetter than, the Evan Jones Mine flora of Alaska, and wetter still than the mid-latitude lowland and upland floras.

It is important to note that the Eocene polar forests would have experienced periods of 24-hour night and day during the respective polar winter and summers, just as modern high-latitude ecosystems do. It has been suggested that due to the low angle solar radiation prevalent at these latitudes during the polar summer, that the leaves of dicotyledonous angiosperm trees would have increased in size (Wolfe 1985 and references therein)—effectively eliciting a similar response observed in sun and shade leaves of broad-leaf trees (e.g., Lichtenthaler et al., 1981) and thus introducing a potential source of bias in physiognomic-based precipitation estimates from high latitude ecosystems. However, this hypothesis, and the scale of the potential bias it introduces into physiognomic precipitation estimates, remains untested. Furthermore, data on modern plants across latitudinal bands of 38.1–71.25 °N is equivocal, with increases in mean leaf size, decreases

Deleted: .1

Deleted: 4.5

Deleted: , ranging from 131–180 cm a⁻¹, with a mean value of ~162 cm a⁻¹ (Table 2)

Deleted: ,

in mean leaf size, or no change recorded for broad-leaf trees and shrubs (*Betula* and *Ledum*), and the herbaceous *Arabidopsis* (Kudo, 1995; Hopkins et al., 2008; Migalina et al., 2010).

The climate reconstruction for the Canadian Arctic is in stark contrast to the modern-day climate of Ellesmere and Axel Heiberg islands. Ellesmere Island currently experiences a harsh Arctic desert climate (e.g., Eureka, Nunavut MAT -19.7 °C, CMMT -38.4 °C, WMMT 5.7 °C, MAP 8 cm a⁻¹, 3WET 4 cm, 3DRY < 1 cm; Environment Canada, 2020). These high-latitude paleoclimate estimates for the Canadian Arctic generally agree with previous high latitude proxy climate data from similarly aged deposits (Table 3, Fig. 5). However, the physiognomic, BA, and ensemble estimates of this study typically have cooler MAT values, and wetter MAP values than estimates based on stable isotopes or palynofloras (Table 3). Nevertheless, the temperature estimates of this and previous studies indicate that MAT remained relatively homogenous across the high latitudes throughout the late Paleocene and into the early Eocene (Fig. 5).

4.2 The Latitudinal Temperature Gradient in northern North America

The latitudinal temperature gradient is considered a defining characteristic of the climate system both past and present (Zhang et al., 2019), and is one of the principal factors that control the distribution of vegetation. As such, the persistence of a shallow latitudinal temperature gradient during the early Eocene would have been instrumental in supporting the expansive forest ecosystems that stretched from the mid- to high latitudes (Greenwood and Wing, 1995). An understanding of the latitudinal temperature gradient during warm periods in Earth's history remains an integral component of paleoclimate modelling, and relevance of past megathermal intervals as useful analogs for modern global warming (Greenwood and Wing, 1995; Naafs et al., 2018).

However, climate models have had difficulty replicating the shallow latitudinal temperature gradient of the early Eocene (Hollis et al., 2019), with temperatures either unrealistically hot in the tropics, or too cold at the poles and continental interiors. The most successful of these models required $p\text{CO}_2$ of 4480 ppm, which is on the extreme upper end of early Eocene estimates, although CO_2 calibrations tend to lose sensitivity at high values, making quantification difficult (Huber and Caballero, 2011). Paleobotanical proxy methods have been criticized, as differing methods can produce different results (Hollis et al., 2019); however, the ensemble climate estimate method offers considerable improvements for estimating past temperature and precipitation regimes over any single method (e.g., Reichgelt et al., 2018; Lowe et al., 2018; Willard et al., 2019). Therefore, it is important to re-evaluate the latitudinal temperature gradient for northern North America as methodological improvements are made and new data become available.

The modern latitudinal temperature gradient for north-western North America is approximately 1.2 °C/1° latitude (Greenwood and Wing 1995). Previously, paleobotanical data from the Western Interior of North America had been used to estimate the latitudinal temperature gradient, which suggested a latitudinal temperature change of 0.30–0.40 °C/1° latitude for the late

Deleted: 7.6

Deleted: 3.8

Deleted: 0.82

Deleted: -

Deleted: -

Deleted: s

Paleocene and early Eocene (Greenwood and Wing, 1995; Davies-Vollum, 1997). In addition, prior studies used $\delta^{18}\text{O}$ data from coastal marine bivalves to estimate a latitudinal temperature change of $0.28\text{ }^{\circ}\text{C}/1^{\circ}$ latitude for the late Paleocene and early Eocene in North America (Tripathi et al., 2001; Quan et al., 2012, and references therein). Recently, a temperature data compilation of terrestrial climate proxies for the late Paleocene and early Eocene was used to reconstruct a global average latitudinal temperature gradient of $0.16\text{ }^{\circ}\text{C}/1^{\circ}$ between 30° – 60° paleolatitude (Zhang et al., 2019).

As the Okanagan Highlands floras introduce an altitudinal influence, they are not included in an evaluation of the latitudinal temperature gradient. Rather, the temperature estimates from the coastal lowland Racehorse Creek floras are more appropriate for comparison to the lowland floras of higher latitudes. The ensemble estimates of the lowland Racehorse Creek fossil flora ($\sim 48^{\circ}$ N) provides a MAT value of $\sim 19\text{ }^{\circ}\text{C}$. The mean of the ensemble MAT estimates from Ellesmere Island ($\sim 80^{\circ}$ N), NU, Canada is $\sim 10\text{ }^{\circ}\text{C}$. The difference in latitude between the two lowland regions is about 31° , which results in a temperature change per degree of latitude of $0.28\text{ }^{\circ}\text{C}/1^{\circ}$ latitude. The Evan Jones Mine flora (MAT $\sim 13\text{ }^{\circ}\text{C}$) is located geographically between the lowland fossil localities of Racehorse Creek and Ellesmere Island, and as such appears to indicate that the latitudinal temperature gradient is steeper from the mid-latitudes and shallower in the polar latitudes. The latitudinal temperature gradient estimate of $0.28\text{ }^{\circ}\text{C}/1^{\circ}$ latitude corroborates estimates previously derived from both paleobotanical and coastal marine sources (Davies-Vollum, 1997; Tripathi et al., 2001; Quan et al., 2012). Similar northern hemisphere temperature gradients ($0.27\text{ }^{\circ}\text{C}/1^{\circ}$ latitude) have been estimated from fossil plants for the late Paleocene in China (Quan et al., 2012), which indicate that relatively similar temperature gradients may have been in place globally in the northern hemisphere during the late Paleocene and early Eocene.

Deleted: comparable

4.3 Paleobiomes of northern North America

During the early Eocene, subtropical and temperate forests dominated the mid-latitudes and were comprised of a high diversity of both temperate and thermophilic taxa—with thermophilic floral and faunal elements extending poleward in the Eocene, reaching 70°N or more (Eberle and Greenwood, 2012). Vegetation models suggest the mid-latitudes were dominated by mixed deciduous and evergreen forests, which is in broad agreement with fossil evidence (Beerling and Woodward, 2001; Shellito and Sloan, 2006). The ability of models calibrated from modern vegetation dynamics to produce results that broadly agree with the fossil record may suggest that ecophysiological controls on plant distributions have not changed markedly during the Cenozoic (Beerling and Woodward, 2001); however, there is still a need to provide a refined and evidence-based interpretation of the forest ecosystems that were in place in northern North America during the early Eocene.

CLAMP climate results for the mid-latitude lowland and upland fossil localities, as well as the high-latitude lowland sites, plot as temperate forest and temperate rainforest biomes (Fig. 3b) respectively, but group more tightly within the temperate forest biome when BA climate data are plotted (Fig. 3c). Plotting the ensemble climate estimates from northern North America on biome

661 diagrams (Fig. 3b), however, further demonstrates the similarity in both vegetation and climate
662 throughout these regions. The majority of the fossil localities plot within the climate space to be
663 classified as temperate forest ecosystems (Fig. 3), with two high-latitude localities plotting on the
664 boundary between temperate forest and temperate rainforest ecosystems. Whipsaw Creek, a fossil
665 locality of the Okanagan Highlands (Table 1), plots as a grassland biome; however, when the upper
666 end of the errors are considered, this fossil locality overlaps with the fossil localities plotted as
667 temperate forests.

668 Temperature and precipitation correlate positively with the rate of productivity in a forest
669 (Whittaker, 1975). Therefore, the standing biomass and annual net primary productivity of a forest
670 will differ depending on the climatic zone. Typically, temperate forests have an average above-
671 ground net primary productivity (ANPP) of about 9.5 Mg ha⁻¹ yr⁻¹ (Saugier et al., 2001), but this
672 value can differ based on the regional climate. For example, temperate rainforests from the Pacific
673 Northwest with MAP values of > 150 cm a⁻¹ have been shown to have an above-ground biomass
674 of 467–1316 Mg ha⁻¹ and an annual net primary productivity of 4.2–15 Mg ha⁻¹ yr⁻¹ (Gholz, 1982),
675 whereas wetland forests such as the *Taxodium* (swamp cypress) dominated forests of Florida, have
676 been shown to have an above-ground biomass of 284 Mg ha⁻¹ and an ANPP of 16.1 Mg ha⁻¹ yr⁻¹
677 (Brown, 1981). Temperate broad-leaved forests from Tennessee typically have an above-ground
678 biomass of 326–471 Mg ha⁻¹ and an ANPP of 6.3–13.1 Mg ha⁻¹ y⁻¹ depending on the age of the
679 forest stand (Busing, 2013). Biomass and ANPP has been previously reconstructed as 501–587 Mg
680 ha⁻¹ and 5.8–7.8 Mg ha⁻¹ yr⁻¹, respectively, for the late Paleocene to early Eocene *Metasequoia*
681 (dawn redwood) dominated swamp forests of Stenkul Fiord (Williams et al., 2009). Above-ground
682 biomass has also been reconstructed as 946 Mg ha⁻¹ for the middle Eocene forests on Axel Heiberg
683 Island (Basinger et al., 1994). These values fall within the range of values appropriate for modern
684 temperate forests, and the lower to middle range for the temperate rainforests of the Pacific
685 Northwest, which suggests that modern values of biomass and ANPP may be useful
686 approximations for model simulations if the forest biome is known.

687 Our data support previous studies that have described the upland fossil megaf flora of British
688 Columbia and Washington state as having a dominant temperate component, or belonging to a
689 temperate forest ecosystem with analogues from modern west coast temperate forest ecosystems
690 (Greenwood et al., 2016; Lowe et al., 2018). These upland paleofloras reflect forests consisting of
691 mixed temperate and tropical plants, with insects (e.g. lacewings and palm beetles), birds and
692 mammals (e.g. hedgehogs and tapirs) (Archibald et al., 2011; Greenwood et al., 2005, 2016; Eberle
693 et al., 2014; Eberle and Greenwood, 2017). The ancient plant communities were diverse and are
694 typically dominated by taxa such as *Ginkgo*, Pinaceae such as *Pinus* (pine), Cupressaceae such as
695 *Metasequoia* (dawn redwood), *Sassafras*, *Betula* (birch), *Alnus* (alder), *Ulmus* (elm),
696 *Cercidiphyllum/Trochodendroides* (katsura), and rare palms (Smith et al., 2009; DeVore and Pigg
697 2007, 2010; Greenwood et al., 2005, 2016; Mathewes et al., 2016; Lowe et al., 2018). During the
698 early Eocene, more southerly regions of North America hosted mainly tropical flora and fauna,
699 supported by warmer climate conditions than those of the Okanagan Highlands (Archibald et al.,

Deleted: *Picea* (spruce)

2010; Morley, 2011; Eberle and Greenwood, 2012), more similar in climate to the lowland Racehorse Creek flora from western Washington (DeVore and Pigg 2010; Beedlovestrout et al., 2013), fossil floras of the Green River Basin (Wolfe, 1994; Wilf, 2000), and to the southeast (Currano et al., 2010) in the U.S.A.

The lowland Canadian Arctic megafloras have previously been described as representing a temperate rainforest based on leaf physiognomic climate estimates (e.g., Greenwood et al., 2010; West et al., 2015), an interpretation supported by the leaf physiognomic climate estimate biome plots (Fig. 3), and the fossil taxa present (McIver and Basinger, 1999; Eberle and Greenwood, 2012; West et al., 2019). The early Eocene polar broadleaf deciduous fossil forests of Alaska and those of Ellesmere and Axel Heiberg islands in Arctic Canada reflect a mixed temperate flora (*Ulmus*, *Alnus*, *Tetracentron*, *Magnolia*), with some rare tropical elements (palynological evidence for palms found in the ACEX cores; McIver and Basinger, 1999; Sluijs et al., 2009; Sunderlin et al., 2011; Salpin et al., 2018; West et al., 2015, 2019; Willard et al., 2019). Prior vertebrate paleontological studies from the region have shown that these polar environments were also host to a mix of fauna that included alligators and thermophilic forms of, snakes, turtles, large mammals, terror birds, and early primates (Estes and Hutchinson, 1980; McKenna, 1980; Dawson et al., 1993; Eberle, 2005; Eberle et al., 2014).

Results from PCA show that the mid- and high-latitude lowland fossil localities generally plot with the North American and Eurasian floras (Fig. 4b). Despite this, the leaf physiognomy-based HCA indicates that the Arctic fossil floras are physiognomically distinct from modern floras (Fig. 4c). The mid-latitude floras appear to share some leaf physiognomic characteristics with both the Arctic fossil floras and modern floras from the North American west coast (e.g., Oregon, Washington), and east coast (e.g., Florida, South Carolina). The physiognomic distinctiveness of the Eocene Arctic floras from both modern floras and mid-latitude Eocene floras may be due to an ancient environment with no modern analog, due to the extreme abiotic stress from photic seasonality combined with high precipitation and relatively mild temperatures (e.g., West et al. 2015, and references therein). Forests cannot currently occur at such high latitudes, and therefore these physiognomic responses and adaptations have no modern analogue; thus, these polar ecosystems can be referred to as fossil, or extinct ecosystems (West et al. 2015, and references therein). These results, coupled with the ensemble climate estimates, suggest considerable climatic overlap existed between the mid- and high latitudes during the early Eocene. This suggests that the similar climatic regimes, facilitated by a shallow latitudinal temperature gradient, allowed for similar forest ecosystems—both floristically and vegetatively—to exist at both mid- and high latitudes during the early Eocene, despite substantial differences in latitude and photic seasonality.

5 Conclusions

The results of our ensemble approach to climate reconstruction for the mid- and high latitudes of northern North America describe a low latitudinal temperature gradient (0.28 °C/1° latitude) and broad climatic similarity across a large latitudinal range (~30°) during the early

Deleted: a

Deleted: b

Deleted: -

Deleted: -

743 Eocene, although variation in precipitation between the mid- and high latitudes is evident (Fig. 5).
744 This shallow latitudinal temperature gradient supported an extensive forest ecosystem that spanned
745 most of northern North America from Washington, USA to Ellesmere Island, NU, with several
746 genera occurring throughout its entire extent (e.g., *Metasequoia*, *Alnus*, *Ulmus*; see West et al.,
747 2019). The climate estimates derived from the upland fossil floras of the mid-latitude sites in
748 Washington and British Columbia, coupled with biome charts and physiognomic analysis, indicate
749 that these ancient forests ecosystems share physiognomic features with modern temperate forests
750 from the Pacific Northwest. The high-latitude lowland fossil localities from Arctic Canada plot as
751 temperate forests, alongside fossil floras from the mid-latitudes, but exist at the boundary between
752 the climatic range for a temperate forest and temperate rainforest. ~~Nevertheless~~, in the HCA
753 analysis, the physiognomic character of the Arctic forests was dissimilar from modern forest
754 ecosystems, whereas the mid-latitude fossil sites share more physiognomic qualities with modern
755 forests and the early Eocene polar forests—potentially resulting from similar climatic conditions.
756 Despite the antiquity of these forest ecosystems, the PCA analysis of fossil site physiognomy of
757 both the mid- and high-latitude sites demonstrates that these forests broadly group with modern
758 floras from North America and Eurasia.

Deleted: with

Deleted: Although

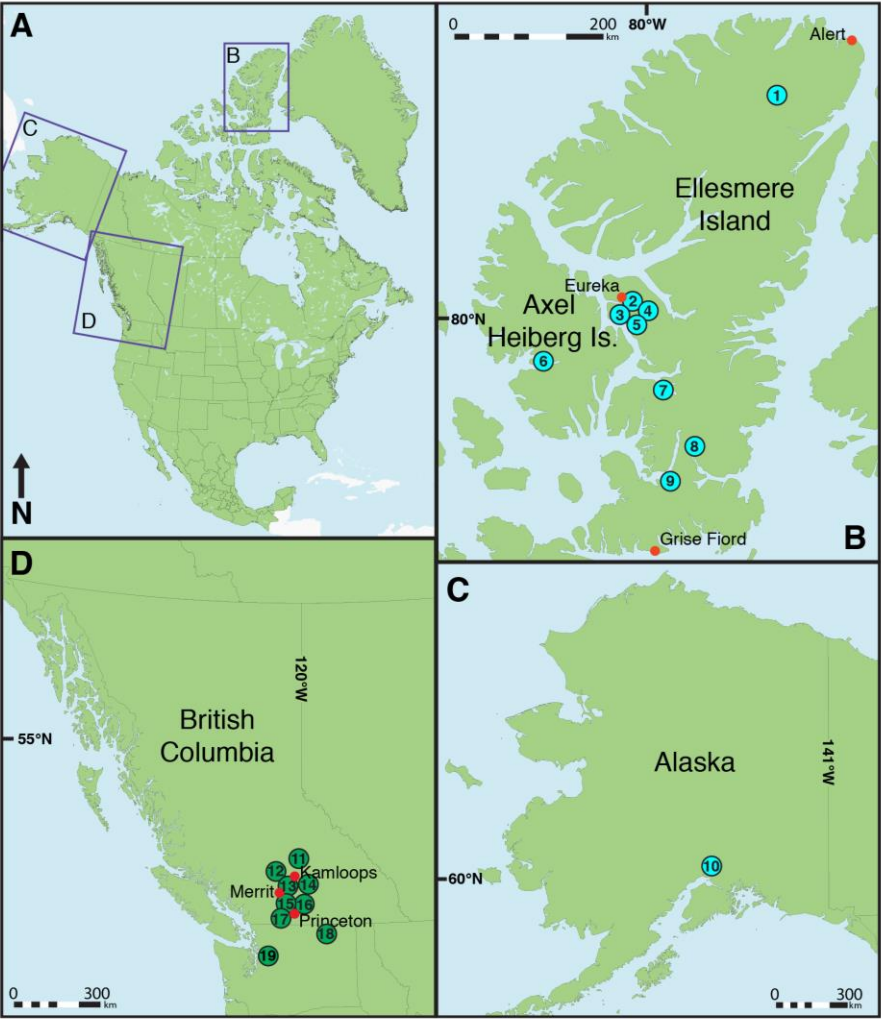
759 These results indicate that the climate of northern North America during the early Eocene
760 was potentially more homogenous than previously appreciated, and capable of supporting
761 climatically, and taxonomically, similar forests at mid- and high latitudes, supported by a shallow
762 latitudinal temperature gradient. Although PCA of the physiognomic character of the Arctic forests
763 broadly groups with modern forest ecosystems, the results of the HCA analysis indicate that these
764 ancient forests do not align physiognomically with any modern forest ecosystem. This is not
765 unexpected, as these high-latitude ecosystems would have experienced pronounced photic
766 seasonality and an enhanced hydrological cycle during Eocene warmth (see West et al., 2015 and
767 references therein)—which resulted in an ecosystem that has since become extinct.

Deleted: , t

768 Improved terrestrial climate estimates and vegetation resulting from an ensemble approach
769 offer opportunities to better classify these ancient forest ecosystems, enhancing utility of the
770 paleobotanical record for paleoclimate modeling. This is a step towards meeting the goals
771 recommended by Hollis et al. (2019) and the modelling community (e.g., DeepMIP; Hollis et al.
772 2019; Lunt et al., 2020) in striving to improve the quality and clarity of proxy data and derived
773 climatic parameters.

774

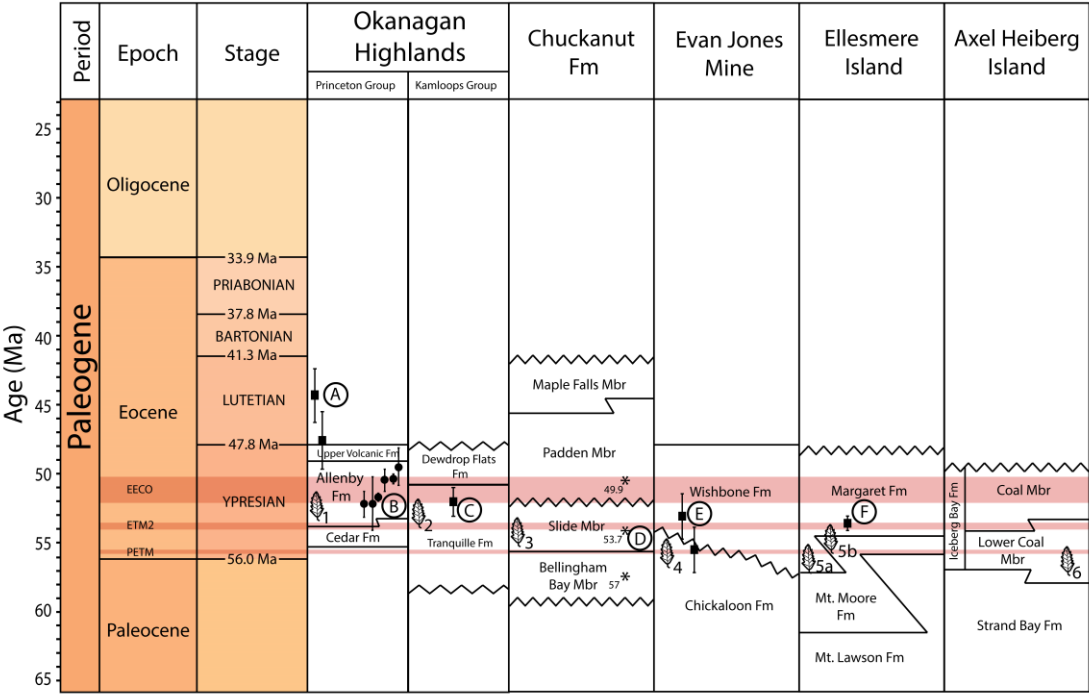
778 Figure 1: Location map showing the location of the fossil localities used in this study. (1) Lake
 779 Hazen, (2) Mosquito Creek, (3) Ox-Head Creek, (4) Hot Weather Creek, (5) Fosheim Anticline,
 780 (6) Strand Fiord), (7) Strathcona Fiord, (8) Split Lake, (9) Stenkul Fiord, (10) Evan Jones Mine,
 781 (11) Chu Chua, (12) McAbee, (13) Quilchena, (14) Falkland, (15) Thomas Ranch, (16) One Mile
 782 Creek, (17) Whipsaw Creek, (18) Republic, (19) Racehorse Creek.



783

784 Figure 2: Stratigraphic compilation of corresponding formations for the fossil localities used in
785 this study. A-F represent the corresponding radiometric data for those formations, and leaf images
786 numbered 1-6 represent approximate stratigraphic positions of the floras used for this study. **Fm =**
787 **Formation; Mbr = Member.** Data compiled from Sunderlin et al., 2011, Breedlovestrout et al.,
788 2013, Greenwood et al., 2016, and West et al., 2015. Modified from West et al., 2019 and
789 Greenwood et al., 2016.

Commented [CW1]: Revised figure.



791 Figure 3: Biome charts showing the paleoclimate data plotted against modern climate parameters
 792 defining modern biomes. (A) Ensemble climate estimates including an inset map of North America
 793 showing locations of modern weather stations, (B) Leaf physiognomy estimates, (C) BA estimates.

Commented [CW2]: Revised figure. Caption modified to reflect the changes.

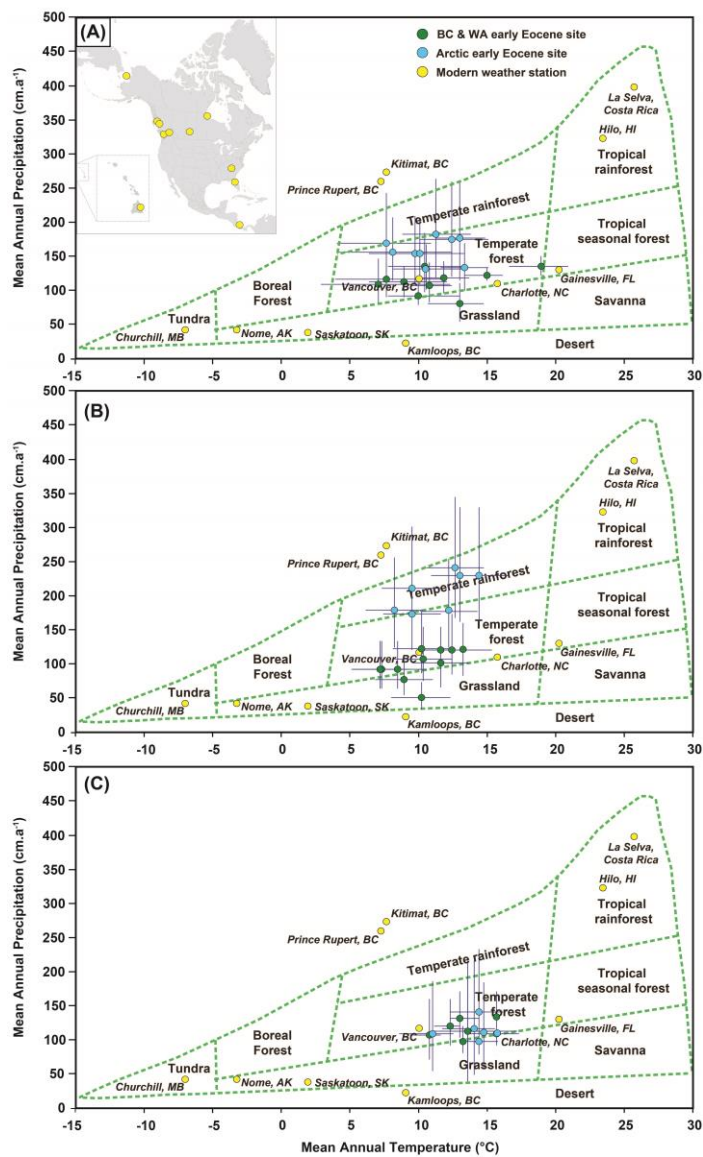
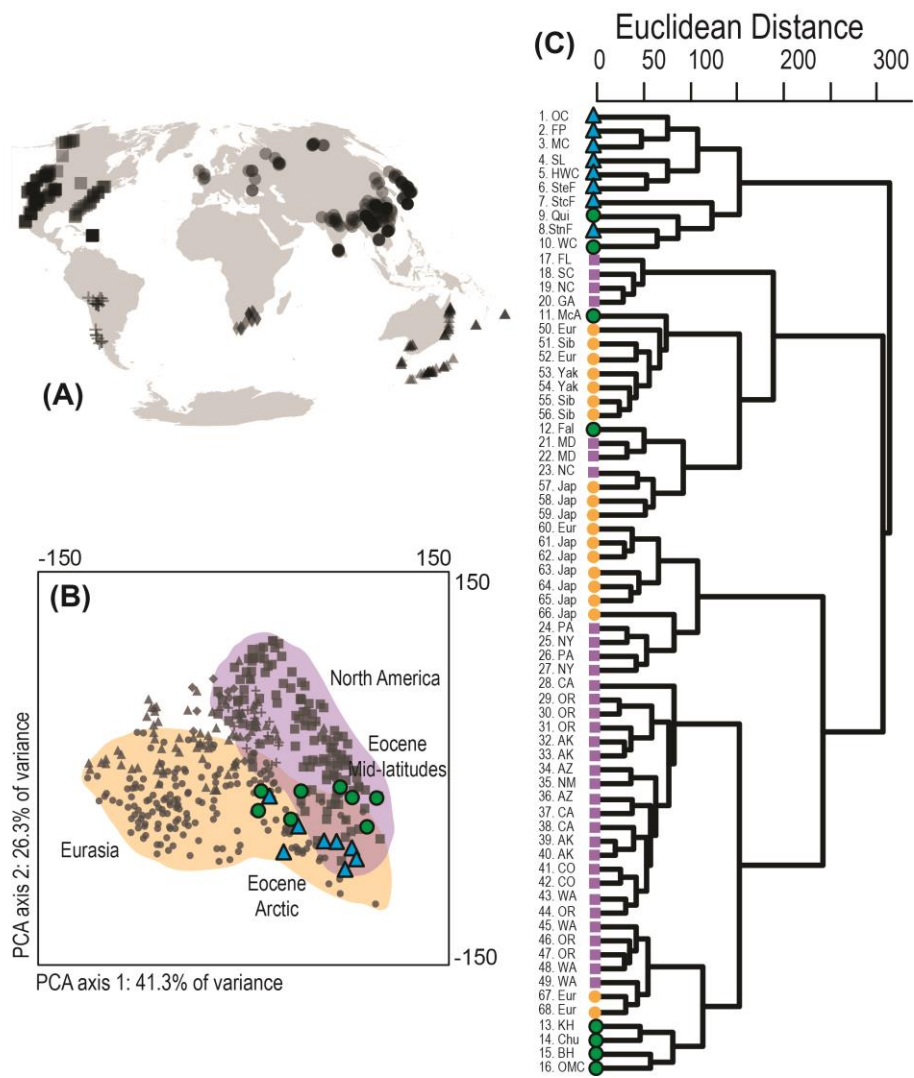


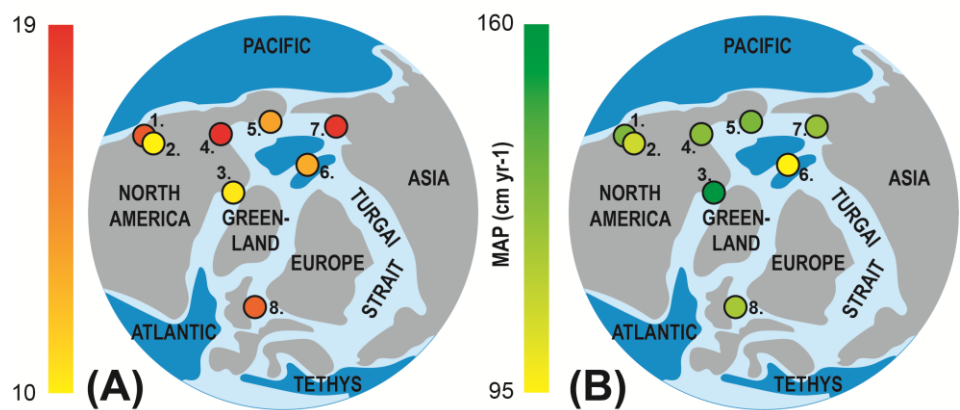
Figure 4: Principal Components Analysis (PCA) and Hierarchical Cluster Analysis (HCA) using CLAMP derived physiognomic data from fossil floras sites from this study and modern sites from clamp.ibcas.ac.cn. (A) Map with location of modern sites in North America (squares), South America (crosses), South Africa (diamonds), Eurasia (circles), and Oceania (pyramids). (B) PCA showing grouping of fossil and modern floras, including the Eocene Arctic (blue pyramids) and the Okanagan Highlands localities (green circles). (C) HCA with selected modern sites, showing the relative similarity between fossil sites from the Eocene Arctic (1. Oxhead Creek, 2. Fosheim Peninsula, 3. Mosquito Creek, 4. Split Lake, 5. Hot Weather Creek, 6. Stenkul Fiord, 7. Strathcona Fiord, 8. Strand Fiord), the Eocene Okanagan Highlands (9. Quilchena, 10. Whipsaw Creek, 11. McAbee, 12. Falkland, 13. Republic Knob Hill, 14. ChuChua, 15. Republic Boot Hill, 16. One Mile Creek), modern North America including Florida (FL), South Carolina (SC), North Carolina (NC), Georgia (GA), Pennsylvania (PA), New York (NY), California (CA), Oregon (OR), Washington (WA), Arizona (AZ), Alaska (AK), New Mexico (NM) and Colorado (CO), 17. Lake George, 18. Simmonsville, 19. Kure Beach, 20. Brunswick, 21. Frederic, 22. SIERC, 23. New Bern, 24. Mt Pocono, 25. Wanakena, 26. Tunkhannock, 27. Lake Placid, 28. Lakeport, 29. Bandon, 30. Port Orford, 31. Nestucca River, 32. Talkeetna, 33. Seward, 34. Greer, 35. Tierra Amarilla, 36. Hasayampa, 37. Blue Canyon, 38. Soda Springs, 39. Eklutna Lake, 40. Sheep Mtn, 41. Wolf Creek, 42. Grand Lake, 43. Bumping Lake, 44. Laurel Mtn, 45. Pt Grenville, 46. Hood River, 47. Troutdale, 48. Wind River, 49. Rimrock Lake) and modern Eurasia including Europe (Eur), Siberia (Sib) and Yakutsk (Yak) (50. Mys Martian, 51. Vagai River, 52. Pogostische, 53. Khartyryk-Khomo, 54. Viluisk, 55. Khanty-Manslisk, 56. Suklyom River, 57. Zozu-san, 58. Higani Shrine, 59. Yakusugi 1080m, 60. Moscow, 61. Akagawa Spa, 62. Kidogawa 2, 63. Toya-ko, 64. Hanawa-Obono, 65. Kidogawa 1, 66. Suganuma, 67. Forge Valley, 68. Monks Wood).

Commented [CW3]: Revised figure (next page) to include a map and made part C larger and easier to read. Updated figure caption to accompany the revised figure. Figure calls in text have also been updated.

Deleted: (



822 Figure 5: Proxy ensemble data from fossil localities showing (A) MAT and (B) MAP estimates
823 from this study, and prior studies compiled in Table 3. 1. Racehorse Creek, Washington, 2.
824 Okanagan Highlands British Columbia and Washington, 3. Canadian Arctic, Ellesmere and Axel
825 Heiberg islands, Nunavut, 4. Mackenzie Delta, Northwest Territories, 5. Evan Jones Mine, Alaska,
826 6. Lomonosov Ridge, 7. New Siberian Islands, Russia 8. North Sea.



829 Table 1: Locality information of fossil sites discussed in this study. BC – British Columbia,
830 Canada; NU – Nunavut, Canada; WA – Washington, USA; AK – Alaska, USA.

<i>Area</i>	<i>Fossil site</i>	<i>Rock unit</i>	<i>Age</i>	<i>Modern Latitude (°N)</i>	<i>Information sources</i>	
WA	Republic	Klondike Fm _v	early Eocene	48.3	Wolfe et al., 1998; This study; Breedlovestrout 2011; Breedlovestrout et al., 2013	Deleted: .
WA	Racehorse Creek	Slide Mbr, Chuckanut Fm _v	early Eocene	48.4	Wolfe et al., 1998; Greenwood et al., 2016; This study	Deleted: .
BC	One Mile Creek	Allenby Fm _v	early Eocene	49.2	Dillhoff et al., 2013	Deleted: .
BC	Thomas Ranch	Vermillion Bluffs Shale, Allenby Fm _v	early Eocene	49.2	Greenwood et al., 2016; This study	Deleted: .
BC	Whipsaw Creek	Vermillion Bluffs Shale, Allenby Fm _v	early Eocene	49.2	Mathews et al., 2016; This study	Deleted: .
BC	Quilchena	Coldwater Beds	early Eocene	50.1	Smith 2011; Smith et al., 2009, 2012	Deleted: .
BC	Falkland	Tranquille Fm _v	early Eocene	50.3	Gushulak et al., 2016; Lowe et al., 2018	Deleted: .
BC	McAbee	Tranquille Fm _v	early Eocene	50.4	Wolfe et al., 1998; Greenwood et al., 2016; This study	Deleted: .
BC	Chu Chua	Chu Chua Fm _v	early Eocene	51.2	Sunderlin et al., 2011	Deleted: .
AK	Evan Jones Mine	Chickaloon Fm _v	late Paleocene to early Eocene	61.4	West et al., 2015	Deleted: .
NU	Stenkul Fiord	Margaret Fm _v	late Paleocene to early Eocene	77.2	West et al., 2015	Deleted: .
NU	Split Lake	Mt Moore Fm _v	late Paleocene to early Eocene	77.5	West et al., 2015	Deleted: .
NU	Strathcona Fiord	Mt Moore Fm _v	late Paleocene to early Eocene	78.3	West et al., 2019; This study	Deleted: .
NU	Strand Fiord	Iceberg Bay Fm _v	late Paleocene to early Eocene	79.1		Deleted: .

844	NU	Fosheim	?Mt.Moore/?Mar	late Paleocene to	79.4	West et al.,	
		Anticline	garet Fm	early Eocene		2019; This study	Deleted: .
845	NU	Hot Weather	?Mt.Moore/?Mar	late Paleocene to	79.4	West et al.,	Deleted: .
		Creek	garet Fm	early Eocene		2019; This study	Deleted: .
	NU	Mosquito	?Mt.Moore/?Mar	late Paleocene to	79.5	West et al.,	Deleted: .
		Creek	garet Fm	early Eocene		2019; This study	Deleted: .
	NU	Ox-Head	?Mt.Moore/?Mar	late Paleocene to	79.5	West et al.,	Deleted: .
		Creek	garet Fm	early Eocene		2019; This study	Deleted: .
	NU	Lake Hazen	<u>?Mt.Moore/?Mar</u> <u>garet Fm/?Mokka</u> <u>Fiord Fm</u>	late Paleocene to	81.4	West et al.,	
				early Eocene		2019; This study	

850 Table 2: Proxy ensemble climate estimates for fossil plant localities. Bracketed range indicates the
851 95% confidence interval of the bootstrapped paleobotanical proxy estimates. BC – British
852 Columbia, Canada; NU – Nunavut, Canada; WA – Washington, USA; AK – Alaska, USA; BH –
853 Boot Hill; KH – Knob Hill.

<i>Localities</i>	<i>MAT (°C)</i>	<i>WMMT (°C)</i>	<i>CMMT (°C)</i>	<i>MAP (cm a⁻¹)</i>
WA Republic (BH)	7.6 (-0.5-14.3)	18.9 (13.6-24.0)	1.6 (-6.3-7.2)	116 (48-293)
WA Republic (KH)	11.8 (5.0-18.1)	20.6 (17.0-25.2)	2.3 (-5.0-8.7)	118 (51-332)
WA Racehorse Creek	17.3 (10.4-25.4)	23.6 (18.6-28.5)	7.3 (0.3-13.9)	---
WA Racehorse Creek (Landslide)	18.9 (11.6-26.1)	23.1 (19.6-27.8)	11.4 (3.5-17.0)	135 (100-183)
BC One Mile Creek	7.0 (-0.9-13.6)	19.2 (14.6-22.7)	-0.3 (-9.4-5.8)	109 (43-362)
BC Thomas Ranch	9.9 (4.5-13.6)	20.0 (15.9-24.0)	1.1 (-6.8-5.6)	92 (42-140)
BC Whipsaw Creek	13.0 (6.5-21.2)	20.4 (15.8-25.2)	1.2 (-2.8-6.7)	80 (29-244)
BC Quilchena	14.9 (8.10-21.2)	22.7 (18.9-27.1)	5.3 (-1.6-9.8)	121 (62-186)
BC Falkland	10.4 (2.3-15.9)	20.8 (17.4-21.7)	4.3 (-1.5-9.9)	135 (52-416)
BC McAbee	10.8 (4.0-16.7)	20.7 (16.2-27.2)	1.8 (-4.5-8.5)	106 (33-315)
BC Chu Chua	8.9 (1.9-15.0)	18.6 (13.0-21.7)	0.0 (-8.3-5.6)	113 (49-292)
AK Evan Jones Mine	13.3 (7.7-17.6)	21.8 (17.2-26.2)	6.4 (0.8-12.2)	132 (63-367)
NU Stenkul Fiord	11.2 (3.1-17.4)	21.4 (17.6-26.5)	4.0 (-1.8-9.8)	180 (81-549)
NU Split Lake	12.4 (3.4-19.1)	22.2 (13.4-28.8)	3.8 (-5.5-11.2)	174 (63-501)
NU Strathcona Fiord	12.9 (5.2-19.6)	21.8 (18.0-27.1)	4.2 (-1.8-10.5)	175 (78-539)
NU Strand Fiord	10.5 (1.8-17.5)	20.3 (15.7-25.4)	2.7 (-4.4-9.7)	131 (61-374)
NU Fosheim Anticline	10.0 (1.2-16.8)	19.8 (14.0-24.8)	3.1 (-4.7-9.7)	152 (73-442)
NU Hot Weather Creek	9.7 (-0.2-17.0)	20.2 (14.7-25.0)	3.9 (-2.4-11.3)	153 (66-444)
NU Mosquito Creek	7.6 (-0.8-15.0)	18.2 (13.5-23.9)	1.3 (-6.0-7.8)	168 (64-488)
NU Ox Head Creek	8.0 (-1.0-17.0)	19.1 (14.1-24.9)	2.3 (-7.9-11.2)	155 (69-432)

Deleted: a

854

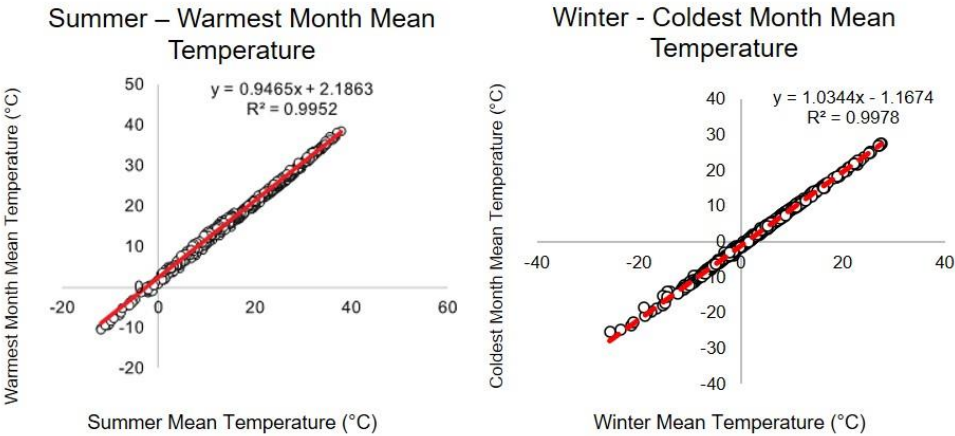
Table 3: Compiled Arctic temperature proxy data from additional [early Eocene](#) sources.

Fossil locality	Age	MAT °C	WMMT °C	CMMT °C	MAP cm a ⁻¹
North Sea ¹	early Eocene	16.0-17.0	~25.0	10.2	>120
Mackenzie Delta ²	late Paleocene to early Eocene	16.0-25.0	25.0-28.0	5.0*15.5	110-160
New Siberian Islands ³	early Eocene	16.0-21.0	25.0-28.0	5.5-14.0	110-140
Lomonosov Ridge ⁴	early Eocene	10.8-14.7	17.9-20.2	3.5-8.9	89.8-97.5

1. Eldrett et al., 2014
2. Salpin et al., 2018
3. Suan et al., 2017
4. Willard et al., 2019

863 **6. Appendix A**

864 Figure A1: Correlation between Summer and Warmest Month Mean Temperature, and Winter and
865 Coldest Month Mean Temperature (Reichgelt et al., 2018). This correlation was used to compare
866 Bioclimatic Analysis results to CLAMP results, as the former uses Summer/Winter Mean, and the
867 latter uses Warmest and Coldest Month Means.



868

869

Table A1: CLAMP derived paleoclimate estimates. Unless otherwise specified, data are original to this study. See Table 1 for locality data. Standard errors and units for climate parameters: MAT $\pm 2.1^{\circ}\text{C}$; CMMT $\pm 3.4^{\circ}\text{C}$; WMMT $\pm 2.5^{\circ}\text{C}$; LGS ± 1.1 months; GSP ± 32 cm; 3-WET ± 23 cm; 3-DRY ± 6 cm; RH $\pm 8.6\%$; SH ± 1.7 g/kg.

Localities	<i>n</i>	MAT	CMMT	WMMT	LGS	GSP	3-WET	3-DRY	RH
WA Republic (Boot Hill)	27	8.5	-0.8	17.9	5.4	74.6	66.1	11.5	66.4
WA Republic (Knob Hill)	43	10.4	0.6	21	6.4	79.9	57.2	15.9	73.2
WA Racehorse Creek (LS)	--	16	8.7	23.6	8.9	123	58.7	23.4	81
WA Racehorse Creek	??	15.3	7.3	23.6	8.6	127	58.7	25.9	82.7
BC One Mile Creek	25	7.2	-3.8	18.5	4.8	48.7	51.5	11.8	69.3
BC Thomas Ranch	31	9	-1.2	20	5.8	68	40	23.3	67.2
BC Whipsaw Creek	36	10.2	-0.3	21.1	6.3	100	65.6	20.5	76.9
BC Quilchena	55	13.3	4.1	23.1	7.7	117	64.7	20.2	76.5
BC Falkland (combined)	70	12.5	4.3	21.7	7.2	85	49.3	28.9	77
BC McAbee	43	11.7	1.3	22.9	6.9	113	65.4	19.9	75.5
BC Chu Chua	27	7.3	-2.5	17.4	4.6	67	62.6	21.2	65.5
AK Evan Jones Mine	??	13.7	6.1	22.2	7.7	118	63.5	36.6	--
NU Stenkul Fiord	25	12.7	3.6	22	7.5	90	46.2	26.5	84
NU Split Lake	11	14.4	4.6	24.4	8.4	96	39.1	31.3	84.2
NU Strathcona Fiord	15	13	4.0	22.3	7.7	111	54.4	27	83.6
NU Strand Fiord	15	10.3	1.0	19.8	6.3	76	52	19.7	79.7
NU Fosheim Anticline	15	9.6	0.8	18.1	6.1	61	44.5	21.8	82.9
NU Hot Weather Creek	10	12.2	3.6	20.8	7.3	80	44.1	25.7	84
NU Mosquito Creek	13	9.5	0.5	18.1	6.1	45	36.9	21.5	83.4
NU Ox Head Creek	13	8.3	-2.1	18.6	5.5	44	37.6	21.2	82.8

n = number of leaf morphotypes scored; MAT = Mean annual temperature; CMMT = Cold month mean temperature; WMMT = Warm month mean temperature; LGS = Length of growing season; GSP = Growing season precipitation; 3-WET = Precipitation during the three consecutive wettest months; 3-DRY = Precipitation during the three consecutive driest months; RH = Relative humidity. BC – British Columbia, Canada; NU – Nunavut, Canada; WA – Washington, USA; AK – Alaska, USA; LS – Landslide.

882 Table A2: Paleoclimate estimates from leaf margin analysis (LMA: Wing & Greenwood
883 1993; Wilf 1997; Peppe et al., 2011) and leaf area analysis (LAA: Wilf et al., 1998; Peppe et al.,
884 2011). Unless otherwise specified, data and estimates original to this study. See Table 1 for locality
885 data. Errors stated within the table; errors for MAP are asymmetric as they are converted from
886 log_e. Where *n* has two values, different *n* applies to LMA/LAA due to overly incomplete leaves
887 being excluded from LAA.

<i>Localities</i>	<i>n</i>	<i>LMP</i>	<i>MAT-1</i>	<i>MAT-2</i>	<i>MLnA</i>	<i>MAP-3</i>	<i>MAP-4</i>
<u>WA</u> Republic (BH)	27	0.07	3.4 ± 1.5	6.1 ± 4.8	6.9	93 +40, -28	130 +109, -59
<u>WA</u> Republic (KH)	43	0.35	11.8 ± 2.2	11.7 ± 4.8	7.1	108 +47, - 33	140 +118, -64
<u>WA</u> Racehorse Ck (LS) ^{††}	32	0.67	21.9 ± 2.6	18.4 ± 4.8	--	--	--
<u>WA</u> Racehorse Creek ^{††}	23	0.61	19.8 ± 3.1	17.0 ± 4.8	--	--	--
<u>BC</u> One Mile Creek	24/25	0.04	2.4 ± 1.2	5.4 ± 4.8	6.9	93 +40, -28	130 +109, -59
<u>BC</u> Thomas Ranch ^{††}	31	0.21	7.8 ± 2.1	--	--	77 +33, -23	--
<u>BC</u> Whipsaw Creek	24	0.46	15.2 ± 3.1	14 ± 4.8	6.1	51 +22, -16	95 +80, - 43
<u>BC</u> Quilchena ^{††}	55	0.49	16.2 ± 2.0	14.6 ± 4.8	--	121 ± 39	--
<u>BC</u> Falkland [*]	59	0.2	7.3 ± 2.0	8.7 ± 4.8	7.4	121 +52, -37	149 +125, -68
<u>BC</u> McAbee [†]	43	0.3	10.2 ± 2.5	10.6 ± 4.8	6.7	87 +76, -8	125 +105, -57
<u>BC</u> Chu Chua	24	0.19	6.9 ± 2.4	8.4 ± 4.8	6.9	93 +40, -28	130 +109, -59
<u>AK</u> Evan Jones Mine [†]	39	0.321	11.0 ± 2.3	--	7.6	155 +108, - 221	--
<u>NU</u> Stenkul Fiord [†]	25	--	8.5 ± 2.6	9.5 ± 4.8	8.6	240 + 104, - 72	211 +178, -96
<u>NU</u> Split Lake [†]	11	--	10.9 ± 4.3	11.1 ± 4.8	8.5	230 +99, -69	207 +174, -94
<u>NU</u> Strathcona Fiord [†]	15	--	12.4 ± 3.8	12.1 ± 4.8	8.5	230 +99, -69	207 +174, - 94
<u>NU</u> Strand Fiord	15/13	0.23	8.2 ± 3.6	9.3 ± 4.8	7.4	123 +53, -37	150 +126, -68,
<u>NU</u> Fosheim Anticline	15	0.2	7.3 ± 3.2	8.7 ± 4.8	8	173 +75, -52	178 +149, -81
<u>NU</u> Hot Weather Creek	10/9	0.15	5.7 ± 3.5	7.7 ± 4.8	8	177 +77, -53	181 +151, -82
<u>NU</u> Mosquito Creek	13/10	0.7	3.3 ± 2.1	6.1 ± 4.8	8.4	210 +91, -63	197 +165, -90
<u>NU</u> Ox-Head Creek	13/11	0.8	3.5 ± 2.3	6.2 ± 4.8	8.1	178 +77, -54	181 +152, -82

888 n = number of dicot leaf morphotypes scored; LMP = leaf margin proportion (number of non-
 889 toothed leaf morphotypes as proportion of n : $0 > X \leq 1.0$; Wilf, 1997); MAT = Mean annual
 890 temperature; MAT-1 = LMA equation of Wing and Greenwood, 1993; MAT-2 = LMA global
 891 equation of Peppe et al., 2011; MLnA = mean leaf size expressed as \log_e ; MAP = mean annual
 892 precipitation, where MAP-3 = LAA equation of Wilf et al., 1998; MAP-4 = LAA global equation
 893 of Peppe et al., 2011. BC – British Columbia, Canada; NU – Nunavut, Canada; WA – Washington,
 894 USA; AK – Alaska, USA; BH – Boot Hill; KH – Knob Hill; LS – Landslide.

895
 896 †† Breedlovestrout et al., 2013.
 897 ‡‡ Dillhoff et al., 2013
 898 ++ Mathewes et al., 2016
 899 * Smith et al., 2011.
 900 + Lowe et al., 2018.
 901 ‡ Sunderlin et al., 2011.
 902 † West et al., 2015.
 903

Table A3: Paleoclimate estimates using NLR-based BA method. BC – British Columbia, Canada; NU – Nunavut, Canada; WA – Washington, USA; AK – Alaska, USA; LS – Landslide.

Localities	<i>min</i> <i>MAT</i>	<i>mean</i> <i>MAT</i>	<i>max</i> <i>MAT</i>	<i>minS</i> <i>umT</i>	<i>mean</i> <i>SumT</i>	<i>maxS</i> <i>umT</i>	<i>minW</i> <i>inT</i>	<i>mean</i> <i>WinT</i>	<i>max</i> <i>WinT</i>	<i>minM</i> <i>AP</i>	<i>mean</i> <i>MAP</i>	<i>max</i> <i>MAP</i>
<u>WA</u> Republic Boot Hill	11.8	13.1	13.9	19.5	21	23.2	2.3	6.0	7.1	112.2	131.8	151.4
<u>WA</u> Republic - Knob Hill	12.7	13.6	14.2	20.2	21.3	22.4	3.2	4.8	7.6	100.0	112.2	131.8
<u>WA</u> Racehorse Ck (Slide Mbr)	18.4	19.4	20.4	22.3	23.6	24.8	13.2	14.3	16.3	114.8	134.9	158.5
<u>BC</u> One Mile Creek	12.0	13.6	13.6	19.8	21.3	22	2.3	4.8	6	97.7	112.2	120.2
<u>BC</u> Thomas Ranch	12.4	13.6	13.6	20.2	21.3	22	2.9	4.8	5.8	97.7	112.2	120.2
<u>BC</u> Whipsaw Creek	10.8	13.3	13.6	18.7	21	22.6	1.0	4.4	6.4	85.1	97.7	128.8
<u>BC</u> Quilchena	15.4	15.7	15.7	23	23	23.7	7.0	7.0	7.7	117.5	131.8	131.8
<u>BC</u> Falkland	12.6	13.6	13.6	20.2	21.3	21.3	4.8	4.8	6.2	102.3	112.2	117.5
<u>BC</u> McAbee	10.0	10.8	12.2	18.2	19.2	21.3	0.8	2.8	5.4	89.1	107.2	128.8
<u>BC</u> Chu, Chua BC	11.8	12.4	13.6	19.8	21.5	22.0	2.2	2.9	5.0	104.7	120.2	13
<u>AK</u> Evan Jones Mine	13.9	14.8	16.4	20.7	23.1	24.0	5.5	7.1	9.6	91.2	109.6	144.5
<u>NU</u> Stenkul Fiord	12.7	13.6	15.6	20.3	21.3	24.2	3.1	4.8	7.7	95.5	112.2	131.8
<u>NU</u> Split Lake	10.0	13.6	15.6	17.3	21.3	24.7	-0.1	4.8	9.0	77.6	112.2	154.9
<u>NU</u> Strathcona	11.1	13.6	15.7	18.4	21.3	24.4	2.0	4.8	8.7	89.1	112.2	151.4
<u>NU</u> Strand Fiord	12.3	13.6	16.0	20.1	21.3	24.1	3.2	4.8	9.0	95.5	112.2	147.9
<u>NU</u> Fosheim Anticline	12.3	14.8	16.0	20.1	23.1	24.7	3.2	7.1	9.1	95.5	109.6	144.5
<u>NU</u> Hot Weather Creek	11.1	13.6	15.7	18.4	21.3	24.3	1.8	4.8	8.9	89.1	112.2	154.9
<u>NU</u> Mosquito Creek	9.6	11.1	13.6	17.3	19.1	22.6	-0.5	3.9	6.7	81.3	109.6	147.9
<u>NU</u> Oxhead Creek	12.6	14.1	16.4	18.8	20.3	23.7	4.8	8.1	10.4	95.5	117.5	144.5
<u>NU</u> Lake Hazen	12.6	14.4	16.4	19.5	22.2	24.0	3.9	6.9	9.8	95.5	141.3	144.5

Deleted: a

minMAT = minimum mean annual temperature; *meanMAT* = average mean annual temperature; *maxMAT* = maximum mean annual temperature; *minSumT* = minimum summer temperature; *meanSumT* = average summer temperature; *maxSumT* = maximum summer temperature; *minWinT* = minimum winter temperature; *meanWinT* = average winter temperature; *maxWinT* = maximum winter temperature; *minMAP* = minimum mean annual precipitation; *meanMAP* = average mean annual precipitation; *maxMAP* = maximum mean annual precipitation.

7. Author contributions

CKW and DRG conceived the study. CKW led the writing and co-ordinated the analyses. CKW, JMV, AJL, and JFB collected the samples, and CKW, TR, AJL and JMV collected and analysed the data. CKW, DRG, and JFB wrote the paper with inputs from all of the authors.

919 8. Competing interests

920 The authors declare that they have no conflicts of interest.

921 10. Acknowledgements

922 Field work in B.C. and Arctic Canada was under scientific and paleontological collection permits
923 issued by the B.C. and Nunavut governments where required. DRG and JMV thank K. Pugh for
924 the loan of his Whipsaw Creek fossil collection and for site information. We thank R.Y. Smith and
925 R.L. Love (formerly Breedlovestrout) for the provision of CLAMP analyses from their PhD work.
926 This work includes research from the Doctoral dissertation of CKW at the University of
927 Saskatchewan, and the Master of Science theses of JMV and AJL at Brandon University. DRG,
928 CKW and TR thank D. Lunt, C. Hollis and M. Huber for suggestions on the scope of the paper.

929 Financial support. This work was substantially supported by: the Natural Sciences and Engineering
930 Research Council of Canada (NSERC) through Discovery Grants (DG 311934 and 2016-04337)
931 to DRG, a Doctoral Scholarship (Alexander Graham Bell Doctoral Scholarship) to CKW; a grant
932 from the Brandon University Research Committee to DRG for Arctic field work; Geological
933 Society of America student research grants to CKW (11816-17) and to JMV (12565-19), and
934 Paleontological Society and SEPM graduate awards to AJL, and a National Geographic Society
935 Exploration Grant (9652-15) to DRG (S.B. Archibald and J. Eberle co-PIs), and a Vetlesen
936 Foundation Climate Center grant to TR, all for field work support in British Columbia. DRG
937 acknowledges support from the Canada Foundation for Innovation (project 31801) and Research
938 Manitoba for laboratory facilities at Brandon University used in this study, and Brandon University
939 Student Union for student employment grants for two B.C. field seasons. Arctic fieldwork by JFB
940 was supported by NSERC (DG 1334) and the Polar Continental Shelf Program.

941 11. References

- 942 Archibald, S.B., Bossert W.H., Greenwood D.R., and Farrell B.D.: Seasonality, the latitudinal
943 gradient of diversity, and Eocene insects, *Paleobiology*, 36, 374-398, 2010.
- 944 Archibald, S.B., Greenwood, D.R., Smith, R.Y., Mathewes, R.W., and Basinger, J.F.: Great
945 Canadian Lagerstätten 1. Early Eocene Lagerstätten of the Okanagan Highlands (British
946 Columbia and Washington State), *Geosci. Can.*, 38(4), 2011.
- 947 Archibald, S.B., Greenwood D.R., and Mathewes R.W.: Seasonality, montane beta diversity, and
948 Eocene insects: testing Janzen's dispersal hypothesis in an equable world, *Palaeogeogr.*
949 *Palaeoclim. Palaeoecol.*, 371,1-8, 2013.
- 950 Archibald, S.B., Morse, G.E., Greenwood, D.R., and Mathewes, R.W.: Fossil palm beetles refine
951 upland winter temperatures in the Early Eocene Climatic Optimum, *Proc. Nat. Academy.*
952 *Sci.*, 111, 8095-8100, 2014.

- Basinger, J. F., Greenwood, D. R., Sweda, T.: Early Tertiary vegetation of Arctic Canada and its relevance to paleoclimatic interpretation. In: Cenozoic plants and climates of the Arctic, Springer, Berlin, Heidelberg, pp. 175-198, 1994
- Barke, J., Abels, H.A., Sangiorgi, F., Greenwood, D.R., Sweet, A.R., Donders, A.F., Reichart, G.J., Lotter, T., and Brinkhuis, H.: Orbitally-forced *Azolla* blooms and middle Eocene Arctic hydrology: Clues from palynology, *Geology*, 39(5), 427 – 430, 2011.
- Beerling, D., and Woodward, F.I.: Vegetation and the terrestrial carbon cycle: the first 400 million years, Cambridge University Press. 2001.
- Breedlovestrout, R.L.: Paleofloristic studies in the Paleogene Chuckanut Basin, Western Washington, USA. PhD dissertation, University of Idaho. 189 pp., 2011.
- Breedlovestrout R.L., Evraets, B.J., and Parrish, J.T.: New Paleogene climate analysis of western Washington using physiognomic characteristics of fossil leaves, *Palaeogeogr. Palaeoclim. Palaeoecol.*, 392, 22–40, 2013.
- Brown, S.: A comparison of the structure, primary productivity, and transpiration of cypress ecosystems in Florida, *Ecol. Monogr.*, 51(4), 403-427, 1981.
- Busing, R.T.: NPP Temperate Forest: Great Smoky Mountains, Tennessee, USA, 1968-1992, R1. Data set. Available on-line [<http://daac.ornl.gov>] from Oak Ridge National Laboratory Distributed Active Archive Center, Oak Ridge, Tennessee, USA. doi:10.3334/ORNLDAAAC/804. 2013.
- Carmichael, M.J., Lunt, D.J., Huber, M., Heinemann, M., Kiehl, J., LeGrande, A., Loptson, C. A., Roberts, C.D., Sagoo, N., Shields, C., Valdes, P.J., Winguth, A., Winguth, C., and Pancost, R.D.: A model–model and data–model comparison for the early Eocene hydrological cycle, *Clim. Past*, 12, 455–481, <https://doi.org/10.5194/cp-12-455-2016>, 2016.
- Carmichael, M.J., Pancost, R.D., and Lunt, D.J.: Changes in the occurrence of extreme precipitation events at the Paleocene–Eocene thermal maximum, *Earth Planet Sc. Lett.*, 501, 24–36, 2018.
- Currano, E. D., Labandeira, C. C., and Wilf, P.: Fossil insect folivory tracks paleotemperature for six million years, *Ecol. Monogr.*, 80, 547-567, 2010.
- Davies-Vollum, K.S.: Early Palaeocene palaeoclimatic inferences from fossil floras of the western interior, USA, *Palaeogeogr. Palaeoclim. Palaeoecol.*, 136, 145-164, 1997.
- Dawson, M. R., McKenna, M. C., Beard, K. C., and Hutchison, J. H.: An early Eocene plagiomenid mammal from Ellesmere and Axel Heiberg islands, Arctic Canada, *S. Kaupia*, 3, 179-192, 1993.
- DeVore, M.L., and Pigg, K.B.: A brief review of the fossil history of the family Rosaceae with a focus on the Eocene Okanogan Highlands of eastern Washington State, USA, and British Columbia, Canada, *Plant Syst. Evol.*, 266, 45–57, 2007.
- DeVore, M.L., and Pigg, K.B.: Floristic composition and comparison of middle Eocene to late Eocene and Oligocene floras in North America, *B. Geosci.*, 85(1), 111–134, 2010.
- DeVore, M.L., and Pigg, K.B.: Paleobotanical evidence for the origins of temperate hardwoods, *Int. J. Plant Sci.*, 174(3), 592–601, 2013.
- Dillhoff, R.M., Dillhoff, T.A., Greenwood, D.R., DeVore, M.L., and Pigg, K.B.: The Eocene Thomas Ranch flora, Allenby Formation, Princeton, British Columbia, Canada, *Botany*, 91, 514-529, 2013.
- Eberle, J.J., and Greenwood, D.R.: An Eocene brontothere and tillodonts (Mammalia) from British Columbia, and their paleoenvironments, *Can. J. Earth Sci.*, 54(9), 981–992, 2017.

999 Eberle, J.J., and Greenwood, D.R.: Life at the top of the greenhouse Eocene world - a review of
 1000 the Eocene flora and vertebrate fauna from Canada's High Arctic, *Geol. Soc. Am. Bull.*,
 1001 124 (1/2), 3–23, doi: 10.1130/B30571.1, 2012.
 1002 Eldrett, J.S., Greenwood, D.R., Harding, I.C., and Huber, M.: Increased seasonality through the
 1003 Eocene to Oligocene transition in northern high latitudes, *Nature*, 459 (7249), 969–974,
 1004 doi: 10.1038/nature08069, 2009.
 1005 Eldrett, J.S., Greenwood, D.R., Polling, M., Brinkhuis, H., and Sluijs, A.: A seasonality trigger
 1006 for carbon injection at the Paleocene–Eocene Thermal Maximum, *Clim. Past*, 10, 759–
 1007 769, doi: 10.5194/cp-10-759-2014, 2014.
 1008 Estes, R. and Hutchison, J. H.: Eocene lower vertebrates from Ellesmere Island, Canadian Arctic
 1009 Archipelago, *Palaeogeog., Palaeoclim., Palaeoecol.*, 30, 325–347, 1980.
 1010 Environment Canada, National Climate Data and Information Archive:
 1011 <http://www.climate.weatheroffice.ec.gc.ca>, last accessed January 2020.
 1012 Gholz, H.L.: Environmental limits on aboveground net primary production, leaf area, and
 1013 biomass in vegetation zones of the Pacific Northwest, *Ecology*, 63, 469–481, 1982.
 1014 Greenwood, D.R.: Fossil angiosperm leaves and climate: from Wolfe and Dilcher to Burnham
 1015 and Wilf. *Cour. Forsch. Senck.*, 258, 95–108, 2007.
 1016 Greenwood, D.R., Archibald, S.B., Mathewes, R.W., and Moss, P.T.: Fossil biotas from the
 1017 Okanagan Highlands, southern British Columbia and northeastern Washington State:
 1018 climates and ecosystems across an Eocene landscape, *Can. J. Earth Sci.*, 42(2), 167–185,
 1019 doi: 10.1139/E04-100, 2005.
 1020 Greenwood, D.R., Basinger, J.F., and Smith, R.Y.: How wet was the Arctic Eocene rainforest?
 1021 Estimates of precipitation from Paleogene Arctic macrofloras, *Geology*, 38(1), 15–18,
 1022 doi: 10.1130/G30218.1, 2010.
 1023 Greenwood, D.R., Pigg, K.B., Basinger, J.F., and DeVore, M.L.: A review of paleobotanical
 1024 studies of the Early Eocene Okanagan (Okanogan) Highlands floras of British Columbia,
 1025 Canada and Washington, U.S.A. *Can. J. Earth Sci.*, 53(6), 548–564, doi: 10.1139/cjes-
 1026 2015-0177, 2016.
 1027 Greenwood, D.R., Keefe, R.L., Reichgelt, T., and Webb, J.A.: Eocene paleobotanical altimetry
 1028 of Victoria's Eastern Uplands, *Aust. J. Earth Sci.*, 64(5), 625–637, 2017.
 1029 Greenwood, D.R., and Conran, J.G.: Fossil coryphoid palms from the Eocene of Vancouver,
 1030 British Columbia, Canada, *Int. J. Plant Sci.*, 181(2), 224–240,
 1031 <https://doi.org/10.1086/706450>, 2020
 1032 Greenwood, D. R., & Wing, S.L.: Eocene continental climates and latitudinal temperature
 1033 gradients, *Geology*, 23, 1044–1048, 1995.
 1034 Grimm, G.W. and Potts, A.J.: Fallacies and fantasies: the theoretical underpinnings of the
 1035 Coexistence Approach for palaeoclimate reconstruction, *Clim. Past*, 12, 611–622,
 1036 <https://doi.org/10.5194/cp-12-611-2016>, 2016.
 1037 Gushulak, C.A.C., West, C.K., and Greenwood, D.R.: Paleoclimate and precipitation seasonality
 1038 of the Early Eocene McAbee megaflora, Kamloops Group, British Columbia, *Can. J.*
 1039 *Earth Sci.*, 53(6), 591–604, doi: 10.1139/cjes-2015-0160, 2016.
 1040 Herold, N., Buzan, J., Seton, M., Goldner, A., Green, J.A.M., Müller, R.D., Markwick, P., and
 1041 Huber, M.: A suite of early Eocene (~ 55 Ma) climate model boundary conditions,
 1042 *Geosci. Model Dev. Disc.*, 7, 2077–2090, <https://doi.org/10.5194/gmd-7-2077-2014>,
 1043 2014.

Deleted: 2019

1045 Hijmans, R.J., Cameron, S.E., Parra, J.L., Jones, P.G., and Jarvis, A.: Very high re-resolution
 1046 interpolated climate surfaces for global land areas, *Int. J. Climatol.* 25, 1965–1978,
 1047 <https://doi.org/10.1002/joc.127>, 2005.

1048 Hinojosa, L.F., Pérez, F., Gaxioloa, A., and Sandoval, I.: Historical and phylogenetic constraints
 1049 on the incidence of entire leaf margins: insights from a new South American model,
 1050 *Global Ecol. Biogeogr.*, 20, 380–390, 2011.

1051 Hollis, C.J., Dunkley Jones, T., Anagnostou, E., Bijl, P.K., Cramwinckel, M.J., Cui, Y., Dickens,
 1052 G.R., Edgar, K.M., Eley, Y., Evans, D., Foster, G.L., Frieling, J., Inglis, G.N., Kennedy,
 1053 E.M., Kozdon, R., Lauretano, V., Lear, C.H., Littler, K., Meckler, N., Naafs, B.D.A.,
 1054 Pälke, H., Pancost, R.D., Pearson, P., Royer, D.L., Salzmann, U., Schubert, B., Seebeck,
 1055 H., Sluijs, A., Speijer, R., Stassen, P., Tierney, J., Tripathi, A., Wade, B., Westerhold, T.,
 1056 Witkowski, C., Zachos, J.C., Zhang, Y.G., Huber, M., and Lunt, D.J.: The DeepMIP
 1057 contribution to PMIP4: methodologies for selection, compilation and analysis of latest
 1058 Paleocene and early Eocene climate proxy data, incorporating version 0.1 of the
 1059 DeepMIP database, *Geosci. Model Dev.*, 12(7), 3149–3206, doi: 10.5194/gmd-2018-309,
 1060 2019.

1061 [Hopkins, R., Schmitt, J., and Stinchcombe, J.R.: A latitudinal cline and response to vernalization](#)
 1062 [in leaf angle and morphology in *Arabidopsis thaliana* \(Brassicaceae\), *New Phytol.*, 179,](#)
 1063 [155–164, doi: 10.1111/j.1469-8137.2008.02447.x, 2008.](#)

1064 Huber, M., and Caballero R.: The early Eocene equable climate problem revisited, *Clim. Past*, 7,
 1065 603–633, 2011.

1066 Huber, M., and Goldner, A.: Eocene monsoons, *J. Asian Earth Sci.*, 44, 3–23, doi:
 1067 10.1016/j.jseas.2011.09.014, 2012.

1068 Hyland, E.G., Huntington, K.W., Sheldon, N.D., and Reichgelt, T.: Temperature seasonality in
 1069 the North American continental interior during the early Eocene climatic optimum, *Clim.*
 1070 *Past. Disc.*, 14(10), 1391–1404, <https://doi.org/10.5194/cp-2018-28>, 2018.

1071 Inglis, G.N., Carmichael, M.J., Farnsworth, A., Lunt, D.J., and Pancost, R.D.: A long-term, high-
 1072 latitude record of Eocene hydrological change in the Greenland region, *Paleogeogr.*
 1073 *Palaeoclim. Palaeoecol.*, 537, 109378, 2020.

1074 Keery, J.S., Holden, P.B., and Edwards, N.R.: Sensitivity of the Eocene climate to CO₂ and
 1075 orbital variability, *Clim. Past*, 14, 215–238, <https://doi.org/10.5194/cp-14-215-2018>,
 1076 2018.

1077 [Kudo, G.: Leaf traits and shoot performance of an evergreen shrub, *Ledum palustre* ssp.](#)
 1078 [decumbens, in accordance with latitudinal change. *Can. J. Bot.* 73: 1451-1456, doi:](#)
 1079 [10.1139/b95-157, 1995.](#)

1080 Lauretano, V., Littler, K., Polling, M., Zachos, J.C., and Lourens, L.J.: Frequency, magnitude
 1081 and character of hyperthermal events at the onset of the Early Eocene Climatic Optimum,
 1082 *Clim. Past*, 11(10), 1313–1324, doi: 10.5194/cp-11-1313-2015, 2015.

1083 Littler, K., Röhl, U., Westerhold, T., and Zachos, J.C.: A high resolution benthic stable-isotope
 1084 record for the South Atlantic: Implications for orbital-scale changes in Late Paleocene-
 1085 Early Eocene climate and carbon cycling, *Earth Planet Sc. Lett.*, 401, 18–30, doi:
 1086 10.1016/j.epsl.2014.05.054, 2014.

1087 Loptson, C. A., Lunt, D. J., and Francis, J.E.: Investigating vegetation-climate feedbacks during
 1088 the early Eocene, *Clim. Past*, 10, 419–436, 2014.

1089 Lowe, A.J., Greenwood, D.R., West, C.K., Galloway, J.M., Reichgelt, T., and Sudermann, M.:
 1090 Plant community ecology and climate on an upland volcanic landscape during the Early

1091 Eocene Climatic Optimum: McAbee fossil beds, British Columbia, Canada, *Paleogeogr.*
 1092 *Palaeoclim. Palaeoecol.*, 511, 433–448, 2018.
 1093 Lunt, D. J., Dunkley Jones, T., Heinemann, M., Huber, M., LeGrande, A., Winguth, A., Loptson,
 1094 C., Marotzke, J., Roberts, C.D., Tindall, J., and Valdes, P.: A model–data comparison for
 1095 a multi-model ensemble of early Eocene atmosphere–ocean simulations: EoMIP, *Clim.*
 1096 *Past*, 8, 1717–1736, 2012.
 1097 Lunt, D.J., Huber, M., Anagnostou, E., Baatsen, M.L., Caballero, R., DeConto, R., Dijkstra,
 1098 H.A., Donnadieu, Y., Evans, D., Feng, R., and Foster, G.L.: The DeepMIP contribution
 1099 to PMIP4: experimental design for model simulations of the EECO, PETM, and pre-
 1100 PETM (version 1.0), *Geosci. Model Dev.*, 10(2), 889–901, 2017.
 1101 Lunt, D. J., Bragg, F., Chan, W.-L., Hutchinson, D. K., Ladant, J.-B., Niezgodzki, I., Steinig, S.,
 1102 Zhang, Z., Zhu, J., Abe-Ouchi, A., de Boer, A. M., Coxall, H. K., Donnadieu, Y., Knorr,
 1103 G., Langebroek, P. M., Lohmann, G., Poulsen, C. J., Sepulchre, P., Tierney, J., Valdes, P.
 1104 J., Dunkley Jones, T., Hollis, C. J., Huber, M., and Otto-Bliesner, B. L.: DeepMIP:
 1105 Model intercomparison of early Eocene climatic optimum (EECO) large-scale climate
 1106 features and comparison with proxy data, *Clim. Past Discuss.*, [https://doi.org/10.5194/cp-](https://doi.org/10.5194/cp-2019-149)
 1107 [2019-149](https://doi.org/10.5194/cp-2019-149), 2020.
 1108 Maechler, M., Rousseeuw, P., Struyf, A., Hubert, M., and Hornik, K.: *cluster: Cluster Analysis*
 1109 *Basics and Extensions*. R package version 2.1.0., 2019.
 1110 Mathewes, R.W.: Climatic conditions in the western and northern Cordillera during the last
 1111 glaciation: paleoecological evidence, *Géogr. Phys. Quatern.*, 45, 333–339, 1991.
 1112 Mathewes, R.W., Greenwood, D.R., and Archibald, S.B.: Paleoenvironment of the Quilchena
 1113 flora, British Columbia, during the Early Eocene Climatic Optimum, *Can. J. Earth Sci.*,
 1114 53, 574–590, 2016.
 1115 Mathewes, R.W., Greenwood, D.R., and Love, R. L. (2020). The Kanaka Creek fossil flora
 1116 (Huntingdon Formation), British Columbia, Canada—paleoenvironment and evidence for
 1117 Paleocene age using palynology and macroflora. *Can. J. Earth Sci.*, 57, 348–365, 2020.
 1118 McInerney, F.A., and Wing, S.L.: The Paleocene-Eocene Thermal Maximum: A perturbation of
 1119 carbon cycle, climate, and biosphere with implications for the future, *Annu. Rev. Earth*
 1120 *Pl. Sci.*, 39, 489–516, 2011.
 1121 McIver, E.E., and Basinger, J.F.: Early Tertiary floral evolution in the Canadian high Arctic,
 1122 *Ann. Miss. Bot. Gard.*, 523–545, 1999.
 1123 McKenna, M.C.: Eocene paleolatitude, climate, and mammals of Ellesmere Island, *Paleogeogr.*
 1124 *Palaeoclimatol. Palaeoecol.*, 30, 349–362, 1980.
 1125 [Migalina, S.V., Ivanova, L.A., and Makhnev, A.K.: Changes of Leaf Morphology in *Betula*](#)
 1126 [pendula Roth and *B. pubescens* Ehrh. along a Zonal–Climatic Transect in the Urals and](#)
 1127 [Western Siberia. *Russ. J. Ecol.*, 41\(4\): 293–301, doi: 10.1134/S106741361004003X,](#)
 1128 [2010.](#)
 1129 Moss, P.T., Greenwood, D.R., and Archibald, S.B.: Regional and local vegetation community
 1130 dynamics of the Eocene Okanagan Highlands (British Columbia Washington State) from
 1131 palynology, *Can. J. Earth Sci.*, 42, 187–204, 2005.
 1132 Morley, R.J.: Cretaceous and Tertiary climate change and the past distribution of megathermal
 1133 rainforests. In *Tropical rainforest responses to climatic change*, Springer, Berlin,
 1134 Heidelberg, pp. 1–34, 2011.
 1135 Naafs, B.D.A., Rohrsen, M., Inglis, G.N., Lähteenoja, O., Feakins, S.J., Collinson, M.E.,
 1136 Kennedy, E.M., Singh, P.K., Singh, M.P., Lunt, D.J., and Pancost, R.D.: High

temperatures in the terrestrial mid-latitudes during the early Palaeogene, *Nat. Geosci.*, 11(10), 766–771, 2018.

National Oceanic and Atmospheric Administration, National Centers for Environmental Information: <https://www.ncdc.noaa.gov/cdo-web/datatools/normals>, last accessed January 2020.

New M., Lister D., Hulme M., and Mankin I.: A high resolution data set of surface of surface climate over global land areas, *Clim. Res.*, 21, 1–25, doi:10.3354/cr021001, 2002.

Peppe, D.J., Royer, D.L., Cariglino, B., Oliver, S.Y., Newman, S., Leight, E., Enikolopov, G., Fernandez-Burgos, M., Herrera, F., Adams, J.M., and Correa, E.: Sensitivity of leaf size and shape to climate: global patterns and paleoclimatic applications, *New Phytol.*, 190(3), 724–739, 2011.

Pigg, K.B., Dillhoff, R.M., DeVore, M.L., and Wehr, W.C.: New diversity among the Trochodendraceae from the Early/Middle Eocene Okanogan Highlands of British Columbia, Canada and northeastern Washington State, United States, *Int. J. Plant Sci.*, 168(4), 521–532, 2007.

Quan, C., Liu, Y. S. C., and Utescher, T.: Paleogene temperature gradient, seasonal variation and climate evolution of northeast China, *Palaeogeogr. Palaeoclim. Palaeoecol.*, 313, 150–161, 2012.

Reichgelt, T., West, C.K., and Greenwood, D.R.: The relation between the global distribution of palms and climate, *Sci. Rep.*, 8(1), 4721, 2018.

Reichgelt, T., Kennedy, E.M., Conran, J.G., Lee, W.G., and Lee, D.E.: The presence of moisture deficits in Miocene New Zealand, *Global Planet. Change*, 172, 268–277, 2019.

Reinhardt, L., Estrada, S., Andrleit, H., Dohrmann, R., Piepjohn, K., von Gosen, W., Davis, D. W. and Davis, B.: Altered volcanic ashes in Palaeocene and Eocene sediments of the Eureka Sound Group (Ellesmere Island, Nunavut, Arctic Canada), *Z. Dtsch. Ges. Geowiss.*, 164, 131–147, 2013.

Reinhardt, L., von Gosen, W., Piepjohn, K., Lückge, A., and Schmitz, M.: The Eocene Thermal Maximum 2 (ETM-2) in a terrestrial section of the High Arctic: identification by U-Pb zircon ages of volcanic ashes and carbon isotope records of coal and amber (Stenkul Fiord, Ellesmere Island, Canada), In: EGU2017, Vienna, Austria, Proceedings 19: 8145, 2017.

Salpin, M., Schnyder, J., Baudin, F., Suan, G., Suc, J.-P., Popescu, S.-P., Fauquette, S., Reinhardt, L., Schmitz, M.D., and Labrousse, L.: Evidence for subtropical warmth in the Canadian Arctic (Beaufort-Mackenzie, Northwest Territories, Canada) during the early Eocene. In: Piepjohn, K., Strauss, J.V., Reinhardt, L., and McClelland, W.C., eds., *Circum-Arctic Structural Events: Tectonic Evolution of the Arctic Margins and Trans-Arctic Links with Adjacent Orogens*, *Geol. S. Am. Sp.*, 541, 1–28, [https://doi.org/10.1130/2018.2541\(27\)](https://doi.org/10.1130/2018.2541(27)), 2018.

Saugier B., Roy J., and Mooney H.A.: Estimations of global terrestrial productivity: converging toward a single number? In: Roy, J., Saugier, B., and Mooney, H.A., eds., *Terrestrial Global Productivity*, San Diego: Academic, 543–57, 2001.

Shellito, C.J., and Sloan, L.C.: Reconstructing a lost Eocene paradise: Part I. Simulating the change in global floral distribution at the initial Eocene thermal maximum, *Global Planet. Change*, 50(1–2), 1–17, 2006.

1181 Sluijs, A., Schouten, S., Donders, T.H., Schoon, P.L., Röhl, U., Reichart, G.J., Sangiorgi, F.,
 1182 Kim, J.H., Sinninghe Damsté, J.S., and Brinkhuis, H.: Warm and wet conditions in the
 1183 Arctic region during Eocene Thermal Maximum 2, *Nat. Geosci.*, 2, 777–780, 2009.
 1184 Smith, R.Y.: The Eocene Falkland fossil flora, Okanagan Highlands, British Columbia:
 1185 Paleoclimate and plant community dynamics during the Early Eocene Climatic Optimum,
 1186 PhD dissertation, University of Saskatchewan. 190 pp, 2011.
 1187 Smith, R.Y., Basinger, J.F., and Greenwood, D.R.: Depositional setting, fossil flora, and
 1188 paleoenvironment of the Early Eocene Falkland site, Okanagan Highlands, British
 1189 Columbia, *Can. J. Earth Sci.*, 46, 811–822, 2009.
 1190 Smith, R.Y., Greenwood, D.R., and Basinger, J.F.: Estimating paleoatmospheric $p\text{CO}_2$ during the
 1191 Early Eocene Climatic Optimum from stomatal frequency of *Ginkgo*, Okanagan
 1192 Highlands, British Columbia, Canada, *Paleogeogr. Palaeoclim. Palaeoecol.*, 293(1–2),
 1193 120–131, doi: 10.1016/j.palaeo.2010.05.006, 2010.
 1194 Smith, R.Y., Basinger, J.F., and Greenwood, D.R.: Early Eocene plant diversity and dynamics in
 1195 the Falkland flora, Okanagan Highlands, British Columbia, Canada, *Palaeobio.*
 1196 *Palaeoenv.*, 92(3), 309–328, doi: 10.1007/s12549-011-0061-5, 2012.
 1197 Stein, R.: The late Mesozoic-Cenozoic Arctic Ocean climate and sea ice history: A challenge for
 1198 past and future scientific ocean drilling, *Paleoceanogr. Paleoclim.*, 34, 1851–1894, doi:
 1199 10.1029/2018PA003433, 2019.
 1200 Sudermann, M., Galloway, J.M., Greenwood, D.R., West, C.K., and Reinhardt, L.:
 1201 Palynostratigraphy of the lower Paleogene Margaret Formation at Stenkul Fiord,
 1202 Ellesmere Island, Nunavut, Canada, *Palynol.*, In review.
 1203 Sunderlin, D., Loope, G., Parker, N.E., and Williams, C.J.: Paleoclimatic and paleoecological
 1204 implications of a Paleocene–Eocene fossil leaf assemblage, Chickaloon Formation,
 1205 Alaska. *Palaios*, 26(6), 335–345, 2011.
 1206 Suan, G., Popescu, S.M., Suc, J.P., Schnyder, J., Fauquette, S., Baudin, F., Yoon, D., Piepjohn,
 1207 K., Sobolev, N.N., and Labrousse, L.: Subtropical climate conditions and mangrove
 1208 growth in Arctic Siberia during the early Eocene, *Geology*, 45(6), 539–542, 2017.
 1209 Team, R. Core: R: a language and environment for statistical computing, version 3.0. 2. Vienna,
 1210 Austria: R Foundation for Statistical Computing, 2019.
 1211 Tribe, S.: Eocene paleo-physiography and drainage directions, southern Interior Plateau, British
 1212 Columbia, *Can. J. Earth Sci.*, 42, 215–230, 2005.
 1213 Tripathi, A., Zachos, J., Marincovich Jr, L., and Bice, K.: Late Paleocene Arctic coastal climate
 1214 inferred from molluscan stable and radiogenic isotope ratios, *Palaeogeogr. Palaeoclim.*
 1215 *Palaeoecol.*, 170, 101–113, 2001.
 1216 Triplehorn, D. M., Turner, D. L., and Naeser, C.W.: Radiometric age of the Chickaloon
 1217 Formation of south-central Alaska: Location of the Paleocene-Eocene boundary, *Geol.*
 1218 *Soc. Am. Bull.*, 95, 740–742, 1984.
 1219 [van Hinsbergen, D.J., de Groot, L.V., van Schaik, S.J., Spakman, W., Bijl, P.K., Sluijs, A.,](#)
 1220 [Langereis, C.G., and Brinkhuis, H.: A paleolatitude calculator for paleoclimate studies.](#)
 1221 [PloS One., 10\(6\), 1–21, 2015.](#)
 1222 West, C.K., Greenwood, D.R., and Basinger, J.F.: Was the Arctic Eocene 'rainforest' monsoonal?
 1223 Estimates of seasonal precipitation from early Eocene megafloras from Ellesmere Island,
 1224 Nunavut, *Earth Planet Sc. Lett.*, 427, 18–30, doi: 10.1016/j.epsl.2015.06.036, 2015.

1225 West, C.K., Greenwood, D.R., and Basinger, J.F.: The late Paleocene and early Eocene Arctic
1226 megaflora of Ellesmere and Axel Heiberg islands, Nunavut, Canada, *Palaeontogr. Abt.*
1227 B., 300(1–6), 47–163, 2019.

1228 Westerhold, T., Röhl, U., Wilkens, R.H., Gingerich, P.D., Clyde, W.C., Wing, S.L., Bowen, G.J.,
1229 and Kraus, M.J.: Synchronizing early Eocene deep-sea and continental records –
1230 cyclostratigraphic age models for the Bighorn Basin Coring Project drill cores, *Clim.*
1231 *Past*, 14, 303–319, doi: 10.5194/cp-14-303-2018, 2018.

1232 Whittaker, R.H.: *Communities and Ecosystems*, 2nd ed., Macmillan, New York, 1975.

1233 Wilf, P.: Late Paleocene–early Eocene climate changes in southwestern Wyoming:
1234 Paleobotanical analysis, *Geol. Soc. Am. Bull.*, 112(2), 292–307, 2000.

1235 Wilf, P.: When are leaves good thermometers? A new case for leaf margin analysis, *Paleobio.*,
1236 23i, 373–390, 1997.

1237 Willard, D.A., Donders, T.H., Reichgelt, T., Greenwood, D.R., Sangiorgi, F., Peterse, F., Nierop,
1238 K.G., Frieling, J., Schouten, S. and Sluijs, A.: Arctic vegetation, temperature, and
1239 hydrology during Early Eocene transient global warming events, *Global Planet. Change*,
1240 178, 139–152, 2019.

1241 Williams, C. J., LePage, B. A., Johnson, A. H., and Vann, D. R.: Structure, biomass, and
1242 productivity of a late Paleocene Arctic forest, *Proc. Acad. Nat. Sci. Phil.*, 158, 107–127,
1243 2009.

1244 Wing, S.L.: Tertiary vegetation of North America as a context for mammalian evolution. In:
1245 Janis, C.M., Scott, K.M., Jacobs, L.L., Gunnell, G.F., and Uhen, M.D., eds., *Evolution of*
1246 *Tertiary Mammals of North America*, 1, 37–65, Cambridge University Press, 1998.

1247 Wing, S.L., and Greenwood, D.R.: Fossils and fossil climates: the case for equable Eocene
1248 continental interiors, *Philos. T. Roy. Soc. B.*, 341, 243–252, 1993.

1249 Wolfe, J.A.: Tertiary plants from the Cook Inlet region, Alaska, *US Geol. Survey Prof. P.*, 398,
1250 1–32, 1966.

1251 Wolfe, J.A.: Distribution of Major Vegetational Types During the Tertiary. In *The Carbon Cycle*
1252 *and Atmospheric CO₂: Natural Variations Archean to Present* (eds E. Sundquist and W.
1253 Broecker), 32, 357–375, 1985.

1254 Wolfe, J.A.: A method of obtaining climatic parameters from leaf assemblages. US Government
1255 Printing Office, (No. 2040-2041), 1993.

1256 Wolfe, J.A.: Tertiary climatic changes at middle latitudes of western North America,
1257 *Palaeogeogr. Palaeoclim. Palaeoecol.*, 108, 195–205, 1994.

1258 Wolfe, J. A., Forest, C. E., and Molnar, P.: Paleobotanical evidence of Eocene and Oligocene
1259 paleoaltitudes in midlatitude western North America. *Geol. Soc. Am. Bull.*, 110, 664–
1260 678, 1998.

1261 Woodward, F.I., Lomas, M.R., and Kelly, C.K.: Global climate and the distribution of plant
1262 biomes, *Philos. T. Roy. Soc. B.*, 359, 1465–1476, 2004.

1263 Yang, J., Spicer, R.A., Spicer, T.E. and Li, C.S.: ‘CLAMP Online’: a new web-based
1264 palaeoclimate tool and its application to the terrestrial Paleogene and Neogene of North
1265 America. *Palaeobio. Palaeoenviro.*, 91(3), 163, 2011.

1266 Yang, J., Spicer, R.A., Spicer, T.E., Arens, N.C., Jacques, F.M., Su, T., Kennedy, E.M., Herman,
1267 A.B., Steart, D.C., Srivastava, G., Mehrotra, R.C., Valdes, P.J., Mehrotra, N.C., Zhou, Z.,
1268 and Lai, J.: Leaf form – climate relationships on the global stage: An ensemble of
1269 characters, *Global Ecol. Biogeogr.*, 24, 1113–1125, 2015.

Deleted:

- 1271 Zachos J.C., Dickens, G.R., and Zeebe, R.E.: An early Cenozoic perspective on greenhouse
1272 warming and carbon-cycle dynamics, *Nature*, 451: 279–283, 2008.
- 1273 Zhang, L., Hay, W. W., Wang, C., and Gu, X.: The evolution of latitudinal temperature gradients
1274 from the latest Cretaceous through the Present. *Earth Sci. Rev.*, 189, 147-158, 2019.